APPLICATION OF DYNAMIC IMAGE ANALYSIS (DIA) FOR CLASSIFICATION OF SOIL GRANULOMETRY

Linzhu Li, Ph.D., A.M.ASCE

NYU Tandon school of Engineering
Civil and Urban Engineering Department

October 06. 2021

NYU | TANDON SCHOOL OF ENGINEERING

Outline of the presentation

1 Scope of this Research

Motivation

- Traditional Sieve analysis is cumbersome, imprecise, and fails to capture particle granulometry (Shape and texture)
- Scanning Electron Microscope (SEM)
- Laser diffraction
- Micro CT scanner
- Dynamic Image Analysis

Goals

- Evaluation of 2D DIA, 3D DIA and μCT for characterizing sand particle granulometry
- Application of NUMERICAL size, shape descriptors for sand classification instead of particle images
- Apply machine learning methods for automatic identification of particles
- Advance State of the Art in particle classification

Introduction to 2D DIA Operations

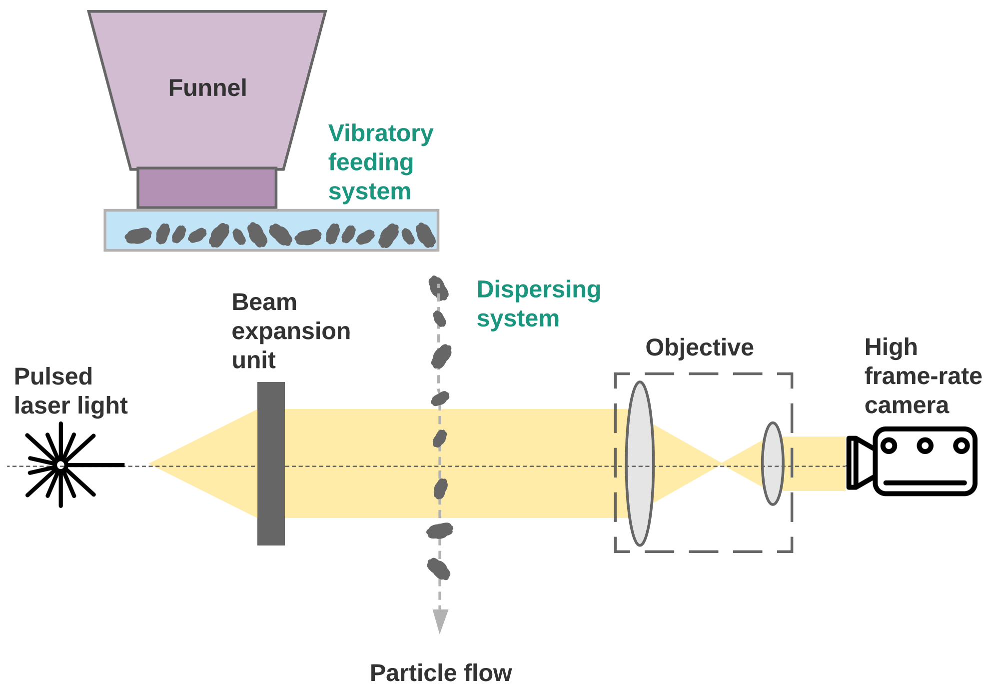

Schematic diagram of 2D DIA

- Multiple images of different particles
- Pulsed laser
- Binary Images

For More Information on 2D DIA

Operating Parameter

- Air pressure
- Moisture content
- Specimen size

Application of DIA to two complex sands

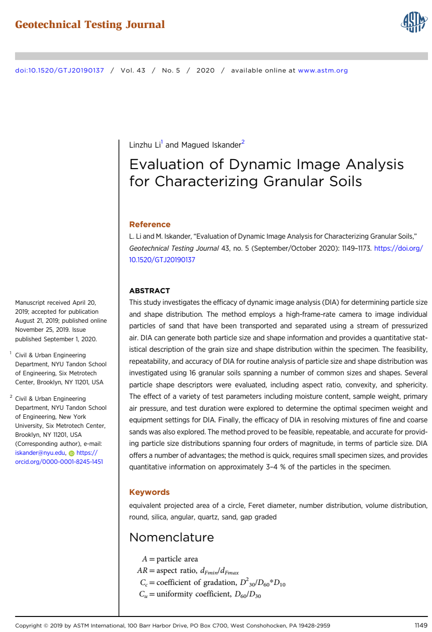

Geotechnical Testing Journal

doi:10.1520/GTJ20190137 / Vol. 43 / No. 5 / 2020 / available online at www.astm.org

Linzhu Li[1] and Magued Iskander[2]

Evaluation of Dynamic Image Analysis for Characterizing Granular Soils

Reference

L. Li and M. Iskander, "Evaluation of Dynamic Image Analysis for Characterizing Granular Soils," *Geotechnical Testing Journal* 43, no. 5 (September/October 2020): 1149–1173. https://doi.org/10.1520/GTJ20190137

Manuscript received April 20, 2019; accepted for publication August 21, 2019; published online November 25, 2019. Issue published September 1, 2020.

1 Civil & Urban Engineering Department, NYU Tandon School of Engineering, Six Metrotech Center, Brooklyn, NY 11201, USA

2 Civil & Urban Engineering Department, NYU Tandon School of Engineering, New York University, Six Metrotech Center, Brooklyn, NY 11201, USA (Corresponding author), e-mail: iskander@nyu.edu, https://orcid.org/0000-0001-8245-1451

ABSTRACT

This study investigates the efficacy of dynamic image analysis (DIA) for determining particle size and shape distribution. The method employs a high-frame-rate camera to image individual particles of sand that have been transported and separated using a stream of pressurized air. DIA can generate both particle size and shape information and provides a quantitative statistical description of the grain size and shape distribution within the specimen. The feasibility, repeatability, and accuracy of DIA for routine analysis of particle size and shape distribution was investigated using 16 granular soils spanning a number of common sizes and shapes. Several particle shape descriptors were evaluated, including aspect ratio, convexity, and sphericity. The effect of a variety of test parameters including moisture content, sample weight, primary air pressure, and test duration were explored to determine the optimal specimen weight and equipment settings for DIA. Finally, the efficacy of DIA in resolving mixtures of fine and coarse sands was also explored. The method proved to be feasible, repeatable, and accurate for providing particle size distributions spanning four orders of magnitude, in terms of particle size. DIA offers a number of advantages; the method is quick, requires small specimen sizes, and provides quantitative information on approximately 3–4 % of the particles in the specimen.

Keywords

equivalent projected area of a circle, Feret diameter, number distribution, volume distribution, round, silica, angular, quartz, sand, gap graded

Nomenclature

A = particle area
AR = aspect ratio, d_{Fmin}/d_{Fmax}
C_c = coefficient of gradation, $D^2_{30}/D_{60}*D_{10}$
C_u = uniformity coefficient, D_{60}/D_{30}

Granulometry of Two Marine Calcareous Sands

Linzhu Li, S.M.ASCE[1]; Ryan D. Beemer, Ph.D., A.M.ASCE[2]; and Magued Iskander, Ph.D., P.E., F.ASCE[3]

Abstract: The morphology of two types of complex calcareous sand was investigated in this study. The materials were selected owing to their different geologic and biologic origins. Ledge Point is a bioclastic coastal sand, while Browse #1 is a hemipelagic sand. These two sands fall outside the range of common data sets used to correlate mechanical properties to particle shape parameters. Morphologic analysis of these calcareous sediments can aid with understanding the engineering behavior of calcareous soils. Moreover, sediments source tracing information could also be inferred from particle shape analysis. Two-dimensional Dynamic Image Analysis (DIA) was employed to capture five million and eight million particle images of each sand, respectively. A number of size parameters including diameter of equivalent projected circle (EQPC), Feret minimum, and Feret maximum diameter were efficiently obtained for each captured image using DIA, and used to investigate particle size distribution of these sediments. In addition, samples of over 800,000 particles were used to assess statistical distributions of various particle shape parameters including Aspect Ratio, Convexity, Sphericity, and Roundness-DIA (by volume). A Johnson family of distributions was found to provide a better fit to particle shape parameter distributions than the normal distribution for both sands. It is also shown that the Sphericity and Aspect Ratio are size independent, while Convexity and Roundness-DIA are correlated with particle size. Convexity is likely correlated with Sphericity for both calcareous sediments owing to their biogenic origin. Correlations of Roundness-DIA, Sphericity, Convexity, and Aspect Ratio and particle size are also observed but need more analysis. **DOI: 10.1061/(ASCE)GT.1943-5606.0002431.** *© 2020 American Society of Civil Engineers.*

Author keywords: Calcareous sediments; Dynamic Image Analysis (DIA); Johnson curve fitting; Carbonate; Particle shape; Roundness; Maximum and minimum void ratio.

Introduction

Calcareous sediments consist mainly of clastic biogenic calcium carbonate from shells and tests (shells of single celled organisms) of marine macro- and microorganisms. As a result, calcareous sands possess complex physical shapes (Beemer et al. 2018). These sediments have been known to be problematic for designing foundations because they exhibit large volume changes and friction angle softening (Murff 1987). In particular, these characteristics have been related to pile running, the tendency of volumetric changes during pile installation to reduce skin friction (Al-Douri and Poulos 1995).

In siliceous sands, strength, compressibility, critical state parameters, hydraulic conductivity, packing density, and void ratio can vary with particle shape (Cho et al. 2006; Rousé et al. 2008; Bareither et al. 2008; Kuo and Freeman 2000; Shin and Santamarina 2013; Zheng and Hryciw 2016a). Previous research proposed linking micromechanical properties with their macromechanical behavior. This has been done by correlating particle shape parameters with void ratio and critical state parameters of sands. Given these advancements, quantitative study of particle shape analyses may be useful for assessing the behavior of calcareous sands.

Three-dimensional (3D) particle shape measurements derived from two orthogonal X-ray images (Hanaor et al. 2016), microcomputed tomography (Alshibli et al. 2015; Fonseca et al. 2012), Synchrotron microcomputed tomography (Afshar et al. 2018), stereo photography (Zheng and Hryciw 2017), or structured light (Sun et al. 2019b) provide the most accurate representation of particle shape. However, 3D measurement of particle shape can be cumbersome, computationally intensive, slow, and expensive for routine geotechnical practice. Although sophisticated techniques have been used to scan and analyze over 19,000 particles at once (Kong and Fonseca 2018), 3D shape analysis is typically limited to sample sizes on the order of 100 grains (Rorato et al. 2019; Maroof et al. 2020). An alternative to these methods is two-dimensional Dynamic Image Analysis (DIA), which can be used to quickly and efficiently analyze the shape parameters of hundreds of thousands to millions of sand grains in a few minutes.

Two-dimensional DIA has been adopted in geotechnical engineering research to provide statistical descriptions of particle size and shape of millions of individual sand grains at a time (Li and Iskander 2020). DIA provides accurate statistics of particle shape by capturing the 2D projected area of a large sample of particles, at a random orientation (White 2003). The method is fast, convenient, and computationally inexpensive, and the image data set is helpful for conducting computer vision research involving size and shape parameters (Sun et al. 2019c; Machairas et al. 2020).

This paper focuses on the particle size and shape analysis of two types of calcareous sands from offshore Western Australia: Browse #1 and Ledge Point. The two sands are representative of different geologies; the first was obtained from a deep-sea site, while the second is representative of a calcareous coastal site (Fig. 1). Five and eight million particle images were used to measure several

[1]Research Assistant, Dept. of Civil and Urban Engineering, New York Univ. Tandon School of Engineering, 6 Metrotech Center, Brooklyn, NY 11201. Email: LL3256@nyu.edu

[2]Assistant Professor, Dept. of Civil and Environmental Engineering, Univ. of Massachusetts Dartmouth, 285 Old Westport Rd., Dartmouth, MA 02747. ORCID: https://orcid.org/0000-0002-9101-5325. Email: rbeemer@umassd.edu

[3]Professor and Chair, Dept. of Civil and Urban Engineering, New York Univ. Tandon School of Engineering, 6 Metrotech Center, Brooklyn, NY 11201 (corresponding author). ORCID: https://orcid.org/0000-0001-8245-1451. Email: Iskander@nyu.edu

Note. This manuscript was submitted on March 13, 2020; approved on August 13, 2020; published online on December 17, 2020. Discussion period open until May 17, 2021; separate discussions must be submitted for individual papers. This paper is part of the ***Journal of Geotechnical and Geoenvironmental Engineering***, © ASCE, ISSN 1090-0241.

J. Geotech. Geoenviron. Eng., 2021, 147(3): 04020171

Introduction to 3D DIA Operations

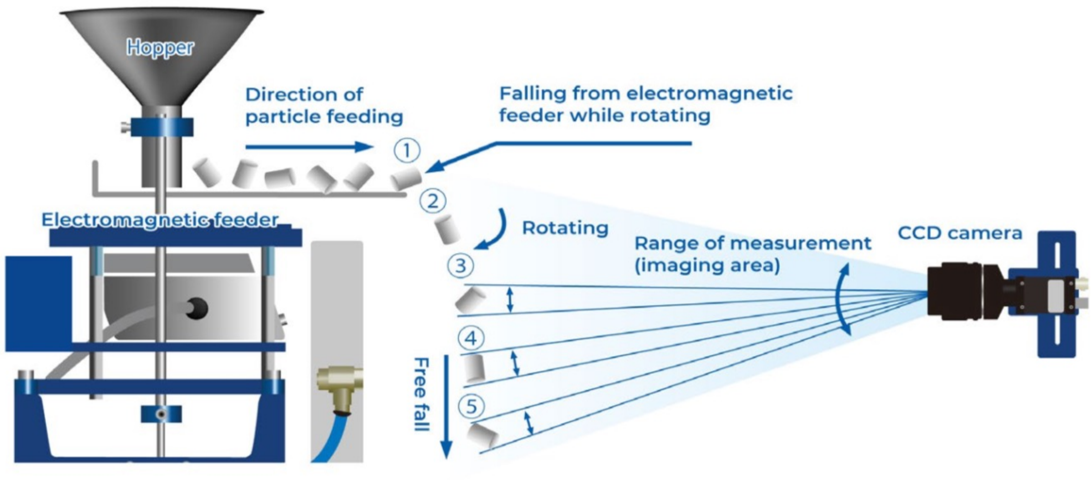

3D DIA - © Microtrac MRB 2020

- Multiple images of same particle
- Gray scale images
- LED light

2 Comparison of 2D & 3D DIA

2D and 3D DIA apparatus

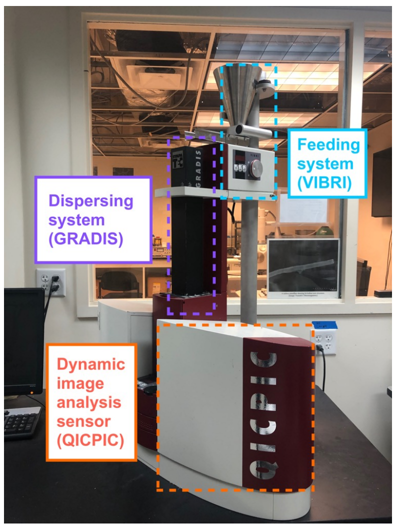

2D DIA apparatus

3D DIA apparatus

	2D DIA	3D DIA
Number of captured images for each particle	one image for each particle from a random plane	takes 8-12 images for each particle
Image resolution	4μm/px	15μm/px
Light source	Pulsed laser	Stroboscopic LED
Frame rate	175 frames/s	100 frames/s
Particle size range	4μm – 10mm	22μm – 35mm
Algorithm	PAQXOS	FLEX
Minimum required particle size for shape analysis	40μm	150μm

3 Materials

19 types of sand

- **Siliceous sand**
  - Ottawa sand: naturally occurring, mechanically sorted, **Rounded**
  - Quartz sand: mechanical crushing of quartzite rock, **Angular**
  - Peace River sand: a natural feldspathic sand sediment, **Subangular and subrounded**
- **Calcareous sand**
  - Marine Sand: hemipelagic sand from a deep-water environment, **Irregular**
  - Beach Sand, coastal bioclastic sand from a shallow-water environment, **Irregular**
  - **Both marine sand sediments contain of Intra-voids**

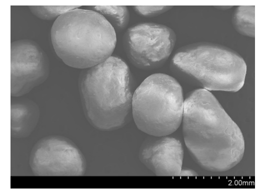
Ottawa #12-20

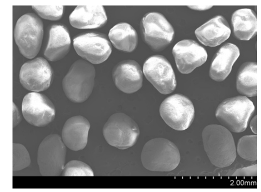
Ottawa #20-30

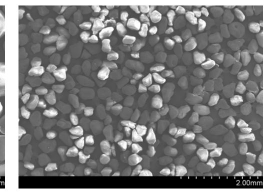
Ottawa #70-100

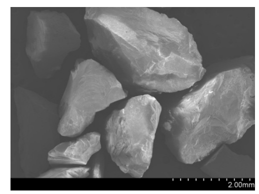
Quartz #4

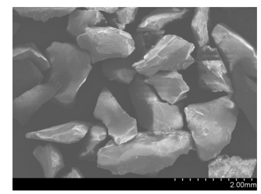
Quartz #3

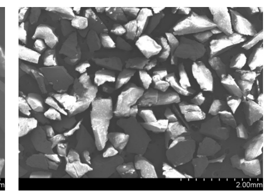
Quartz #2

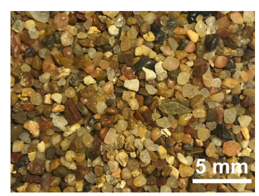

Peace River

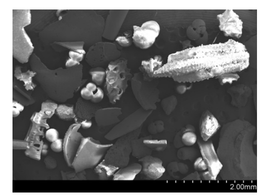
Marine Sand

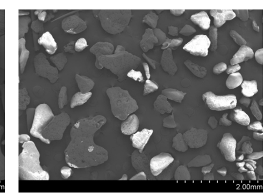
Beach Sand

3 Materials (Images captured by 2D and 3D DIA)

Ottawa #20-30

Peace River

Marine Sand

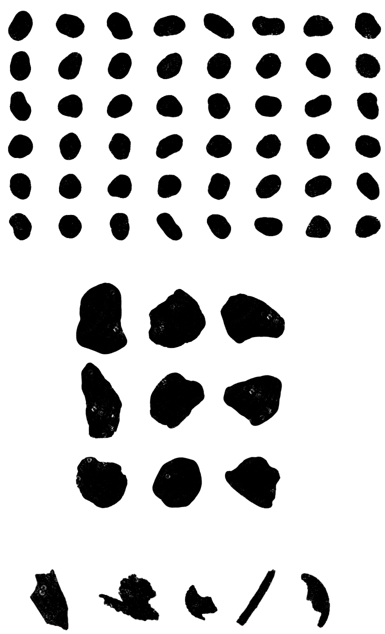

2D DIA

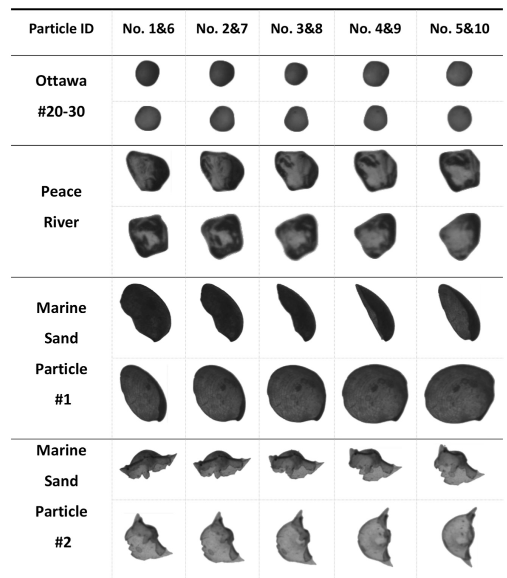

3D DIA

Main difference:

- **2D DIA** captures 1 **binary** particle image at 4μm/px
- **3D DIA** captures 8-12 **grayscale** images of a particle at 15μm/px

4 Particle size and shape descriptors in 2D and 3D DIA

Feret diameter refers to distance between two parallel tangents to the particle at an arbitrary angle:

2D DIA

- d_{Fmax} : longest dimension, d_{Fmin} : shortest dimension

3D DIA

- Feret-length diameter: maximum d_{Fmax} in sequence images
- Feret-width diameter: maximum d_{Fmin} in sequence images
- Feret-thickness diameter: minimum d_{Fmin} in sequence images

EQPC diameter (d_e) is the diameter of a circle with an equal projection area to the particle projection.

In *3D DIA*, d_e = average value in sequence images

Aspect Ratio: *2D DIA*: $AR = \frac{d_{Fmin}}{d_{Fmax}}$; *3D DIA*: $AR_{TL} = \frac{d_{Fthickness}}{d_{Flength}}$;

3D DIA: *Elongation Index* = $\frac{d_{Fthickness}}{d_{Fwidth}}$; *Flatness Index* = $\frac{d_{Fwidth}}{d_{Flength}}$;

3D DIA: *Cx*, *Sp*, *R* = average value in sequence images

Descriptor	Description	2D	3D	Graphically explanation
EQPC (d_e)	Area equivalent circle diameter	$d_e = \sqrt{\frac{4A}{\pi}}$	$d_e = \sqrt{\frac{4\sum_{i=1}^{n} A}{10\pi}}$ A: average Area in sequence of 3D images	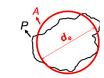
Feret's value (d_{Feret})	Feret diameter	d_{Feret}		
Aspect ratio (AR)	The ratio between minimum Feret diameter to maximum Feret diameter	$AR = \frac{d_{Fmin}}{d_{Fmax}}$	…	
T/L Aspect ratio (AR_{TL})	The ratio between Feret-thickness diameter to Feret-length diameter	…	$AR_{TL} = d_{Fthickness}/d_{Flength}$ Feret-thickness: minimum d_{Fmin} in sequence of 3D images Feret-length: maximum d_{Fmax} in sequence of 3D images	
Elongation Index (EI)	The ratio between Feret-thickness diameter to Feret-width diameter	…	$EI = d_{Fthickness}/d_{Fwidth}$ Feret-thickness: minimum d_{Fmin} in sequence of 3D images; Feret-width: maximum d_{Fmin} in sequence of 3D images;	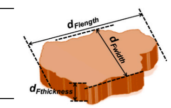
Flatness Index (FI)	The ratio between Feret-width diameter to Feret-length diameter	…	$FI = d_{Fwidth}/d_{Flegnth}$ Feret-width: maximum d_{Fmin} in sequence of 3D images Feret-length: maximum d_{Fmax} in sequence of 3D images	
Convexity (Cx)	The ratio between the projection particle area and the area of the convex hull	$Cx = \frac{A}{A_C}$	$Cx = \frac{\sum_{i=1}^{n} A}{\sum_{i=1}^{n} Ac}$ A: average Area of a sequence of 3D images Ac: average convex hull area of a sequence of 3D images	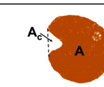
Sphericity (S)	The ratio of the perimeter of the area equivalent circle to the real perimeter	$S = 2\sqrt{\frac{\pi A}{P^2}}$	$S = 2\sqrt{\frac{n\pi \sum_{i=1}^{n} A}{(\sum_{i=1}^{n} P)^2}}$ Area: average Area of a sequence of 3D images Perimeter: average Perimeter of a sequence of 3D images	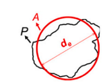
Wadell Roundness (R)	The ratio of the average radius of corner circles of the particle to the radius of the maximum inscribed circle	$R = \frac{\sum_{i=1}^{N} \frac{r_i}{N}}{r_{ins}}$	$R_{3D} = \frac{\sum_{i=1}^{n} R}{n}$ Wadell Roundness = average Roundness of a sequence of 3D images	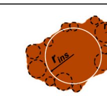

4 Comparison of 2D and 3D DIA

Particle size distribution

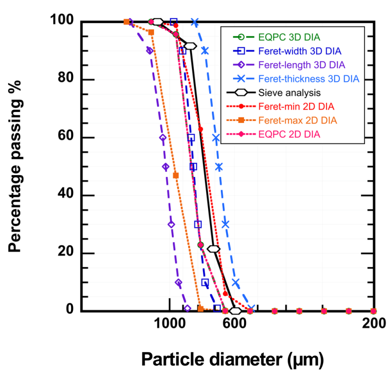

Ottawa #20-30

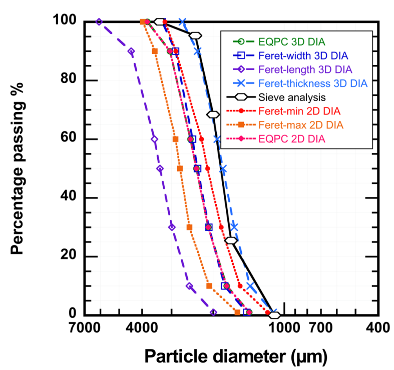

Peace River

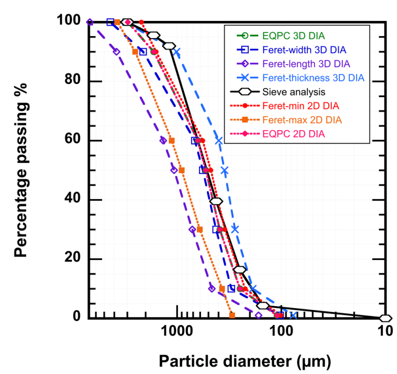

Marine Sand

Particles are assumed to be spheres, and the diameters of these spheres are calculated using selected size descriptors

- The PSD: $d_{Flength} > d_{Fmax} > d_{Fmin} > d_{Fthickness}$
- The PSD of EQPC in 2D DIA and 3D DIA is consistent.
- The PSD of $d_{Fthickness}$ and d_{Fmin} matched with sieve analysis
- Higher image quality is not necessarily required for size analysis.

4 Comparison of 2D and 3D DIA

Particle shape distribution

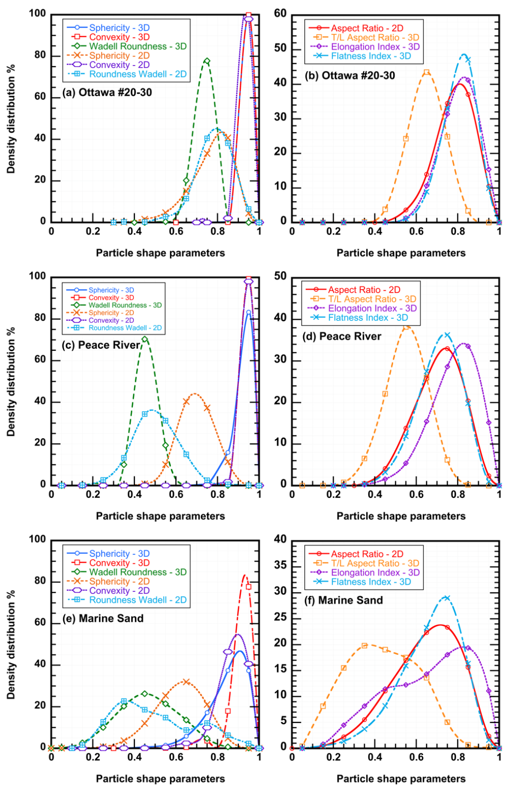

- The standard deviations of *S*, *Cx*, and *R* in 3D DIA are smaller than 2D DIA, 3D data exhibits a more concentrated trend.
- Image resolution affect the shape descriptors characterization: Sphericity: 3D DIA is 26%-39% larger than 2D DIA.

  Convexity: least sensitive descriptor and not much difference

  Roundness: difference from -5 to 14% between 3D and 2D DIA

  Aspect Ratio: The standard deviations are similar.

$$AR_{TL} < AR \approx EI < FI$$

4 Comparison of 2D and 3D DIA

Minimum number of particles for mean shape descriptor

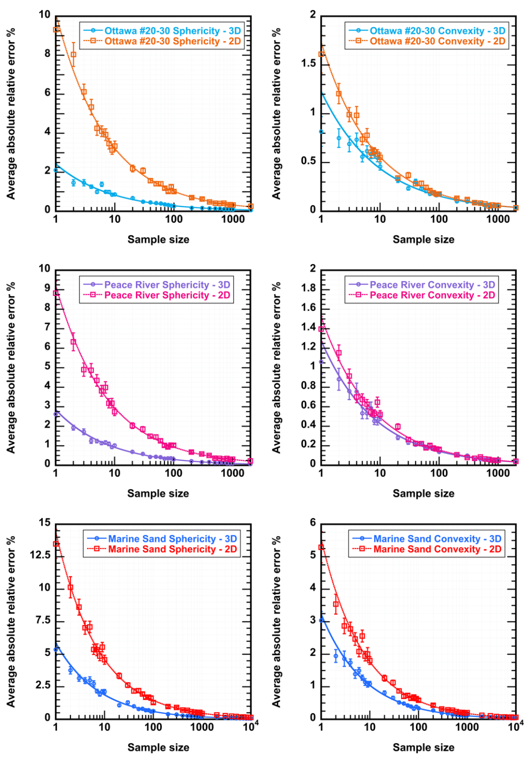

Shape descriptor	Ottawa #20–30		Peace River		Marine Sand	
	2D DIA	3D DIA	2D DIA	3D DIA	2D DIA	3D DIA
Sphericity	400	30	500	40	1000	200
Convexity	20	10	20	8	200	50
Wadell Roundness	…	70	…	300	…	400
Aspect Ratio (AR or T/L)	400	600	600	700	1000	2000
Elongation Index	…	400	…	600	…	2000
Flatness Index	…	500	…	700	…	1000

- Absolute relative error of mean shape value is less than 0.5%
- 2D DIA requires ~10X number of particles than 3D DIA for *S* and *Cx*.
- *Cx* required the least number of particles as 8-50 to represent the entire sample.
- Not much difference for *AR*.

4 Comparison of 2D & 3D DIA

- The operating speed and cost are comparable.
- Particle size is independent of the machines and algorithms.
- Particle shape is sensitive to the technology employed.
- 3D DIA requires a smaller number of sand particles to achieve mean particle shape values.
- 3D DIA provides a more accurate representation of a particles' longest and shortest dimensions.
- Higher resolution of 2D DIA more accurately reflects particle shapes for engineering behavioral analysis.
- Open-source algorithms are helpful in establishing confidence in the computed values

Engineering Geology 290 (2021) 106052

Contents lists available at ScienceDirect

Engineering Geology

journal homepage: www.elsevier.com/locate/enggeo

Comparison of 2D and 3D dynamic image analysis for characterization of natural sands

Linzhu Li, Magued Iskander *

Civil and Urban Engineering Department, NYU Tandon School of Engineering, 6 Metrotech Center, Brooklyn, NY 11201, United States

A R T I C L E I N F O

Keywords:
Granulometry
Elongation index
Flatness index
Johnson coefficients
Zingg and Krumbein chart

A B S T R A C T

The efficacy of Dynamic Image Analysis (DIA) for evaluating particle size and shape parameters was explored using three natural sands, having varying particle morphologies. Two-dimensional (2D) captures binary images of the particles as they free fall in the imaging frame. Although 2D DIA is practical for statistical size and shape analysis, there is a prevailing perception that it fails to fully quantify particle granulometry. In the past few years, 3D DIA has been introduced and has gained acceptance in the pharmaceutical industry. In 3D DIA the system tracks a particle as it falls through the imaging frame and captures gray-scale images from 8 to 12 perspectives of the same particle, and the results are analyzed using average values of these 2D images, which are believed to verge on true particle morphology. Although 2D and 3D devices employ similar methodology they differ in resolution, frame rate, lighting systems, and algorithms. In this work we compare the performance of 2D and 3D DIA. Particle size distributions were expressed using EQPC and a variety of Feret diameters, while particle shape descriptors including Aspect Ratio, Sphericity, Convexity and Roundness were compared for both systems. It is shown that 3D DIA requires a smaller number of sand particles to achieve mean particle shape values. Particle size characterization is generally independent of the machines and algorithms used in this study; however, 3D DIA provides maximum and minimum particle axes which are closer to the real sand particle sizes. Image-based particle shape characterization is more sensitive to the technology employed; it largely depends on image quality, particle angularity, and a hierarchy of shape descriptors; thus, at this time shape analysis for engineering applications must be carried out with similar machines and algorithms. In particular, the image resolutions captured by the available 2D and 3D DIA apparatus are 4 µm and 15 µm per pixel, respectively. At this time, the higher resolution and shorter exposure time of 2D DIA permits particle shape analysis down to particle sizes having D_{50} on the order of 40 µm, while 3D DIA is limited to D_{50} larger than 150 µm. These thresholds will certainly change as technology allows finer resolutions and shorter exposure times. Finally, the importance of image processing cannot be overlooked, and manufacturers and researchers are encouraged to open-source their algorithms in order to establish confidence in them.

1. Introduction

Particle shape has a significant influence on the mechanical behavior of granular soils; therefore, accurate characterization of sand particle morphology is important for predicting the engineering performance of sand (Cho et al. 2006; Cavarretta et al. 2010; Zheng and Hryciw 2016). Generally, the shape of sand particles can be described using two methods: the projection of a particle on a plane (two-dimensional, 2D), or three-dimensional (3D) particle shape which can be obtained using X-ray micro-computed tomography (µCT), among other methods. Although 3D methods provide a richer description of particle morphology, Dynamic Image Analysis (DIA) can be used more efficiently to quickly analyze various particle shape parameters, including Aspect Ratio, Convexity, Sphericity and Roundness of millions of particles (Li et al. 2021).

In recent years, DIA of particle size and morphology has been increasingly applied in geotechnical engineering (e.g. Altuhafi et al. 2016; Bandini et al. 2017; Zhang et al. 2017; Shang et al. 2018; Wang et al. 2019; Wei et al. 2020; Suescun-Florez et al. 2020). DIA employs a high frame-rate camera to image a large number of individual particles of sand in a short time. DIA can generate both particle size and shape distributions and provide a quantitative statistical description of the tested sand. Particle size distribution obtained using DIA shows a good

* Corresponding author.
E-mail addresses: LL3256@nyu.edu (L. Li), Iskander@nyu.edu (M. Iskander).

https://doi.org/10.1016/j.enggeo.2021.106052
Received 17 June 2020; Received in revised form 13 February 2021; Accepted 14 February 2021
Available online 24 February 2021

5 Comparison of 3D DIA and μCT

3D μCT Procedure

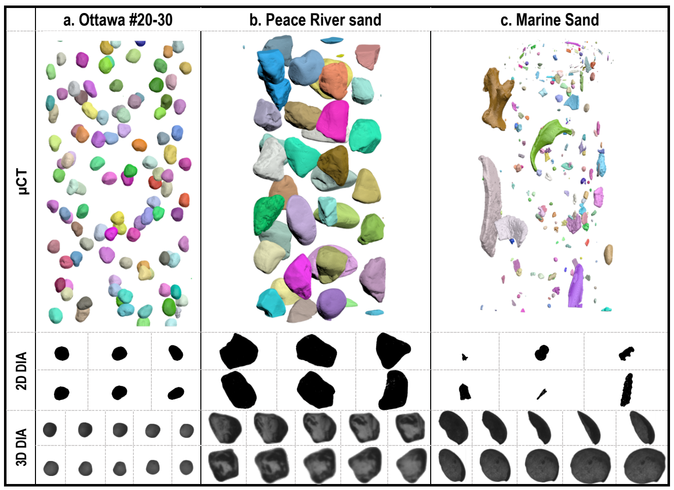

3D particle shape characterization	
Resolution	15μm/voxel
Particle number	110-350 sand particles
Size analysis	300 particles/h
Shape analysis	8 particles/h
Image processing	Voids were filled as solid particle

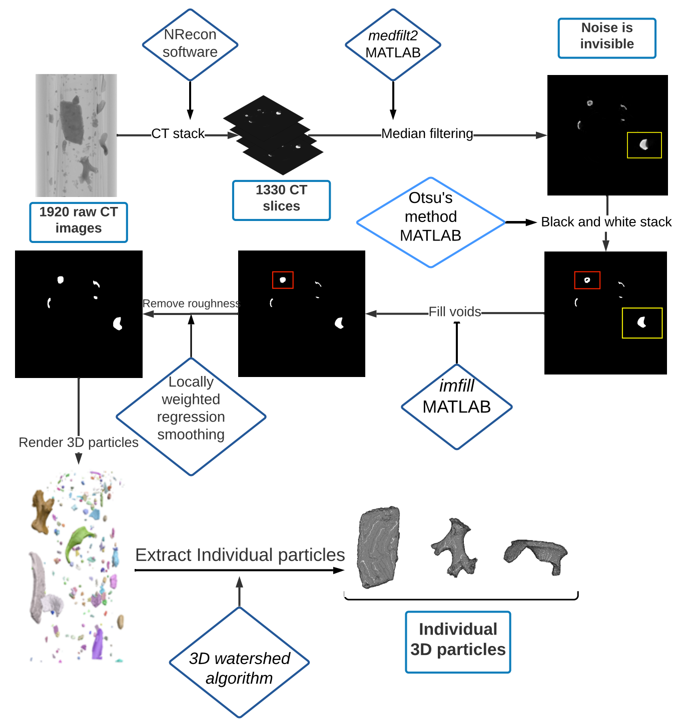

The workflow of CT images post processing for Marine Sand.

5 Comparison of 3D DIA and µCT

3D Particle size and shape descriptors

Size Descriptors	DIA	Formula/Explanation		µCT	Formula/Explanation	
EQPC (d_e)	Diameter of circle with equivalent particle area (2D) or average equivalent diameter from multiple (n‡) views (3D)	$\sqrt{\frac{4A}{\pi}}$ $\sqrt{\frac{4\sum_{i=1}^{n} A}{n\pi}}$	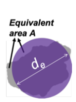	Diameter of sphere with equivalent particle volume	$\sqrt[3]{\frac{6V}{\pi}}$	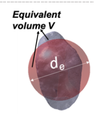
Feret-max† (d_{Fmax})	Maximum dimension of a particle, aka. Maximum Feret diameter (2D)	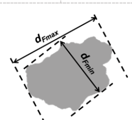		...		
Feret-min (d_{Fmin})	Minimum dimension of a particle, aka. Minimum Feret diameter (2D)			...		
Feret-length ($d_{Flength}$)	Maximum d_{Fmax} from n images of the same particle in 3D DIA	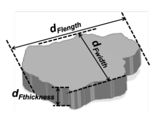		Longest axis ($d_{Flength}$)	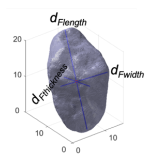	
Feret-width (d_{Fwidth})	Maximum d_{Fmin} from n images of the same particle in 3D DIA			Intermediate axis (d_{Fwidth})		
Feret-thickness ($d_{Fthickness}$)	Minimum d_{Fmin} from n images of the same particle in 3D DIA			Shortest axis ($d_{Fthickness}$)		

Shape Descriptor	DIA	Formula	Graphical Explanation	µCT	Formula	Graphical Explanation
T/L Aspect Ratio (AR_{TL})	Ratio of Feret-thickness to Feret-length (3D)	$\frac{d_{Fthickness}}{d_{Flength}}$	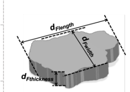	Ratio of shortest to longest axes	$\frac{d_{Fthickness}}{d_{Flength}}$	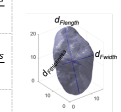
Elongation Index (EI)	Ratio of Feret-thickness to Feret-width (3D)	$\frac{d_{Fthickness}}{d_{Fwidth}}$		Ratio of shortest to intermediate axes	$\frac{d_{Fthickness}}{d_{Fwidth}}$	
Flatness Index (FI)	Ratio of Feret-width to Feret-length (3D)	$\frac{d_{Fwidth}}{d_{Flength}}$		Ratio of intermediate to longest axes	$\frac{d_{Fwidth}}{d_{Flength}}$	
Sphericity (S)	Ratio of the perimeter of a circle with equivalent area to the real particle perimeter (2D) or average equivalent Sphericity from multiple views (3D)	$\frac{\pi d_e}{P}$ $2\sqrt{\frac{n\pi\sum_{i=1}^{n} A}{(\sum_{i=1}^{n} P)^2}}$	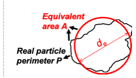	Ratio of the surface area of a volume equivalent sphere to the real particle surface area	$\frac{\pi {d_e}^2}{Sa}$	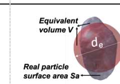
Convexity (Cx)	Ratio between the particle area and the area of its convex hull (2D) or average equivalent convexity from multiple views (3D)	$\frac{A}{Ac}$ $\frac{\sum_{i=1}^{n} A}{\sum_{i=1}^{n} Ac}$	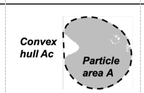	The ratio between the particle volume and the volume of its convex hull	$\frac{V}{V_C}$	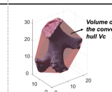
Roundness (R)	Ratio of the average radius of corner circles of the particle to the radius of the maximum inscribed circle (2D) or average equivalent 2D Roundness from multiple views (3D)	$R_{2D\text{-}DIA} = \frac{\sum_{i=1}^{N} \frac{r_i}{N}}{r_{ins}}$ $R_{3D\text{-}DIA} = \frac{\sum_{i=1}^{n} R_{2D-DIA}}{n}$	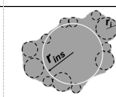	Ratio of the average radius of corner spheres of a particle to the radius of the maximum inscribed sphere	$R = \frac{\sum_{i=1}^{N} \frac{r_i}{N}}{r_{ins}}$	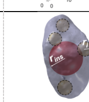

- **Three axes ($d_{Flength}$, d_{Fwidth}, $d_{Fthickness}$)**: perpendicular in µCT but not perpendicular in 3D DIA
- **Shape descriptor dimensionality**: Sphericity and Convexity characterized in 3D DIA and µCT are differed in dimensionality

5 Comparison of 3D DIA and μCT

Particle size distribution

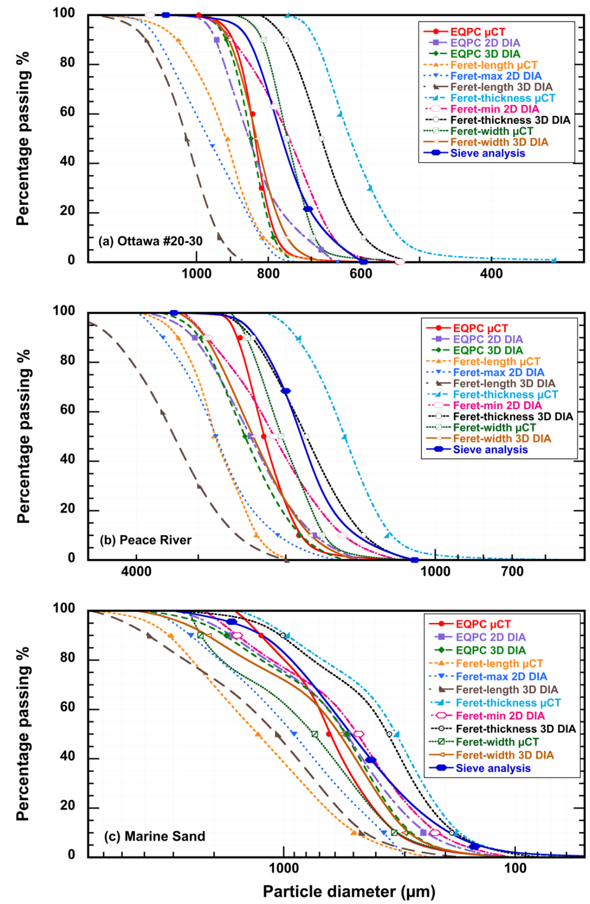

- For rounded particles, EQPC is consistent in 2D, 3D DIA and μCT.
- The differences between 3D DIA and μCT size measurements are approximately 12% on average.
- 3D DIA overestimates the Feret-thickness diameters relative to μCT by 4-19%, 8-12 images cannot capture minimum particle dimension.
- 3D DIA overestimates the Feret-length diameters.

5 Comparison of 3D DIA and µCT

Particle size distribution

Particle size difference
between µCT and 3D DIA

Sand type	Typical particle size	EQPC	Feret-length	Feret-thickness	Feret-width
Ottawa #20-30	D_{10}	0	-12%	-10%	-8%
	D_{30}	0	-11%	-10%	-9%
	D_{50}	-1%	-12%	-8%	-9%
	D_{60}	-2%	-11%	-8%	-9%
	D_{90}	-3%	-9%	-10%	-10%
Peace River	D_{10}	1%	-9%	-10%	-5%
	D_{30}	-5%	-16%	-14%	-11%
	D_{50}	-8%	-17%	-16%	-12%
	D_{60}	-10%	-19%	-18%	-13%
	D_{90}	-17%	-26%	-19%	-17%
Marine Sand	D_{10}	13%	8%	-4%	11%
	D_{30}	19%	16%	-9%	20%
	D_{50}	20%	21%	-8%	30%
	D_{60}	10%	20%	-7%	38%
	D_{90}	-29%	-19%	-5%	8%

Particle size difference between
µCT, 3D DIA and sieve analysis

Sand type	Typical particle size	EQPC	Feret-length	Feret-thickness	Feret-width	EQPC	Feret-length	Feret-thickness	Feret-width
		µCT				3D DIA			
Ottawa #20-30	D_{10}	21%	26%	-17%	7%	21%	43%	-9%	16%
	D_{30}	13%	22%	-19%	1%	14%	37%	-10%	11%
	D_{50}	7%	16%	-20%	-3%	8%	32%	-13%	6%
	D_{60}	6%	18%	-19%	-3%	8%	33%	-12%	7%
	D_{90}	8%	29%	-17%	-1%	11%	42%	-8%	10%
Peace River	D_{10}	57%	91%	4%	41%	56%	110%	16%	49%
	D_{30}	29%	58%	-13%	16%	36%	87%	2%	30%
	D_{50}	17%	47%	-20%	8%	27%	77%	-4%	22%
	D_{60}	14%	43%	-21%	6%	27%	77%	-4%	22%
	D_{90}	3%	37%	-22%	-1%	23%	85%	-3%	20%
Marine Sand	D_{10}	76%	162%	-5%	75%	55%	143%	-1%	58%
	D_{30}	75%	195%	-10%	81%	46%	155%	-1%	50%
	D_{50}	28%	158%	-35%	47%	7%	113%	-30%	13%
	D_{60}	15%	171%	-39%	55%	4%	126%	-34%	12%
	D_{90}	25%	207%	-4%	129%	77%	281%	1%	111%

- These percentage difference may be used as empirical correction factors in engineering practice for similar sands.

5 Comparison of 3D DIA and μCT

PSD calculated using various volume assumptions

- The accuracy of all image-based PSD depends on the volume of the particle obtained from a 2D image:
  - <u>*2D DIA*</u>: volume = $\frac{4}{3}\pi\left(\frac{de}{2}\right)^3$
  - <u>*3D DIA*</u>: volume = $d_{Flength} \times d_{Fwidth} \times d_{Fthickness}$
  - <u>*μCT*</u>: volume = “real” particle volumes
- Only μCT data is used to investigate the volume difference.
- For regular shaped particles, 3D DIA measurement of PSD can represent true volume distribution.
- Volume estimation in 2D DIA resulted in a difference around 3%.
- Volume of irregular particles cannot be reconstructed by three axes obtained from 3D DIA.

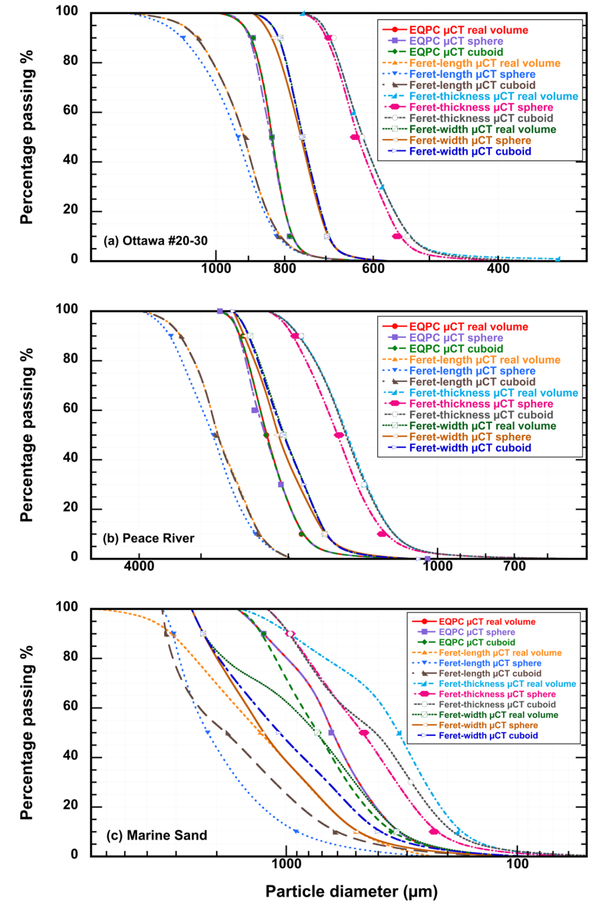

5 Comparison of 3D DIA and μCT

Particle shape distribution

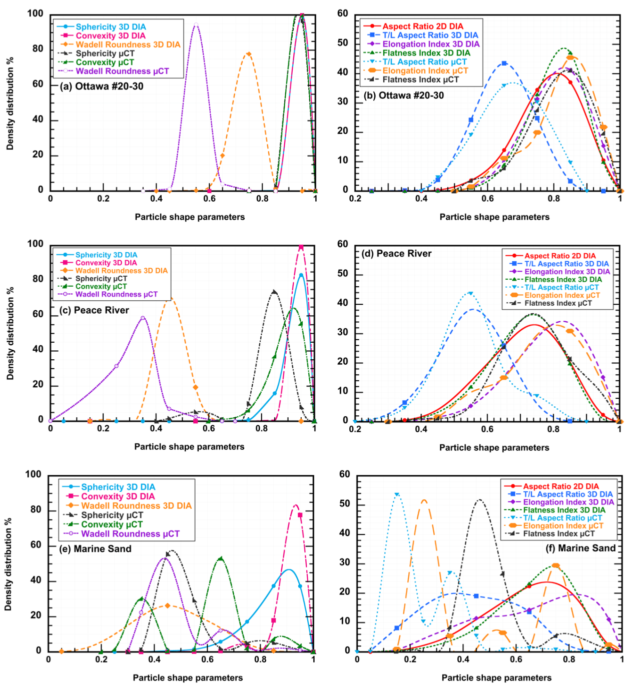

Particle shape distribution using 6 shape descriptors

3D DIA and μCT:

- For Sphericity and Convexity:
  - Ottawa #20-30: 3D DIA ≈ μCT
  - Peace River: differing by 0.1
- For Roundness: μCT < 3D DIA.
- Corner circles in 2D projections are always equal or larger than the corner spheres lodged in 3D volume.
- *R:* μCT is a more objective parameter.
- *R:* 3D DIA is subjected to the projected direction.
- For AR_{TL}, *EI* and *FI*: 3D DIA ≈ μCT
- For complex calcareous sand: 3D DIA ≠ μCT

5 Comparison of 3D DIA and µCT

Differences between 3D DIA and µCT

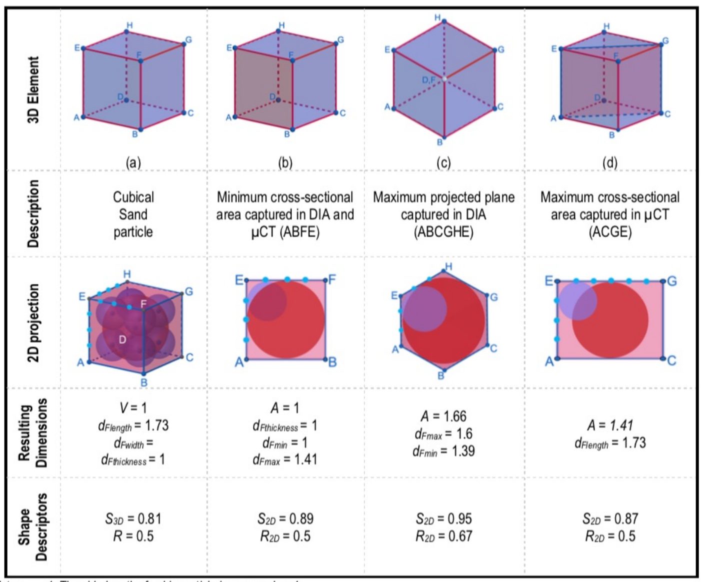

Notes: 1. *The side length of cubic particle is assumed as 1*
2. *The side length of projective plane c is 0.8, which is measured using GeoGebra 3D Calculator.*
3. *The radius of corner circle was calculated using uniform unit pixel per Zheng and Hryciew 2015.*

A hypothetical simple cubic particle

- 3D particles projected into 2D images: projection deformation
- The diameters of corner circles are in direct proportion to the angle between two intersecting lines at the corner.
- The maximum 2D particle area captured by DIA could be larger than the true cross-sectional area.
- *S* and *R* are largest in hexagonal form.
- *S* and *R* are smallest in 3D shape analysis (µCT).

5 Comparison of 3D DIA and μCT

Correlation between 2/3D DIA and μCT

- ➢2D *S*, *Cx* and *R*: calculated using one and ten random projections of the μCT rendering of each particle.
- ➢3D *S*, *Cx* and *R* are calculated from the 3D reconstruction.
- ➢Correlations of *S* and *Cx* increased when employing 10 images (*R* = 0.84±0.13 versus 0.66±0.14).
- ➢3D DIA better represents particle.
- ➢Roundness: No significant correlation.

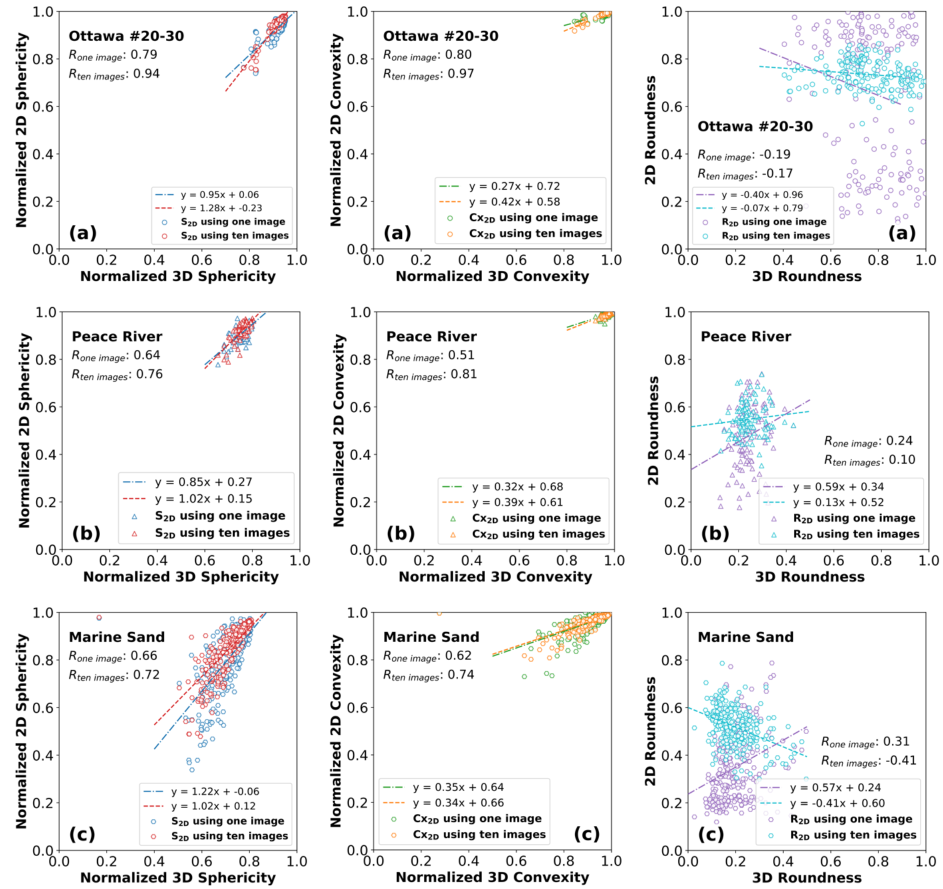

5 Which method to choose?

- **The accuracy** decreases with particle irregularity in 3D DIA .
- **Particle volumes** calculated in 3D DIA provide higher accuracy compared to 2D DIA.
- The ***S*** and ***Cx*** measured in 3D DIA were 2–11% larger compared to µCT. Primary factors (1). dimensionality projection (2). limited number of images.
- The algorithm of **Roundness** in 3D DIA calculated using arithmetic mean values from multiple images result in larger values.

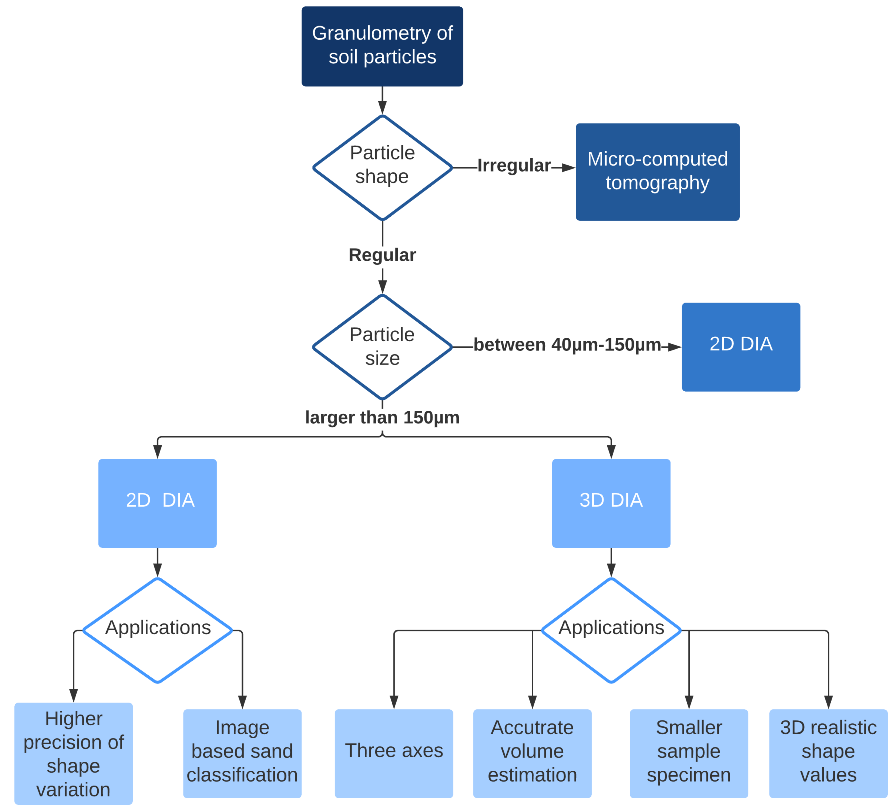

5 For more information

Géotechnique

Efficacy of 3D Dynamic Image Analysis for Characterizing the Morphology of Natural Sands

GEOT-2021-128 | Paper

Submitted on: 26-05-2021

Submitted by: Linzhu Li, Quan Sun, Magued Iskander

Keywords: GRANULOMETRY, MICRO-CT TOMOGRAPHY, COMPUTATIONAL GEOMETRY, DIMENSIONALITY, SANDS

6 Evaluation of roundness parameters in use for sand

Commonly used sphericity and roundness descriptors

Descriptors	Formula/Symbol	Definition	Reference
EQPC	d_e	Diameter of a Circle of Equal Projection Area	ASTM F1877-16
Feret-max	d_{Fmax}	Maximum Feret diameter	Kuo and Freeman 2000
Feret-min	d_{Fmin}	Minimum Feret diameter	
MIC diameter	$d_{ins} = 2r_{ins}$	Maximum inscribed circle diameter	Santamarina and Cho 2004
MCC diameter	$d_{cir} = 2r_{cir}$	Minimum circumscribed circle diameter	
PED diameter	d_p	Diameter of a Circle of Equal Perimeter	ISO 9276-6 2008
Wadell Roundness (R_{wadell})	$R_{wadell} = \frac{\sum_{i=1}^{N} \frac{r_i}{N}}{r_{ins}}$	The ratio of the average radius of corner circles of the particle to the radius of the maximum inscribed circle	Wadell 1932
Convexity (Cx) (aka. Solidity)	$Cx = A/A_c$	The ratio between the real particle area (A) and the area of the convex hull (A_c)	Mora and Kwan 2000
Perimeter Sphericity (S_p)	$S_p = P_e/P = d_e/d_p$	The ratio of the perimeter of the area equivalent circle, P_e, to the real perimeter, P	ISO 9276-6 2008
Circularity (Cr) (1/ Roundness Kato)	$Cr = A/A_p = d_e^2/d_p^2$ $R_{Kato} = A_p/A = d_p^2/d_e^2$	The ratio of the area of the particle (A) to the area of the circle having the same perimeter as the particle ($A_p = \pi d_p^2$)	Cox 1927 Kato 2001
Aspect Ratio (AR) (aka. Wadell's Sphericity)	$AR = d_{Fmin}/d_{Fmax}$	The ratio of the width of the particle (d_{Fmin}) to the length of particle (d_{Fmax})	ISO 9276-6 2008
Circle ratio sphericity (S_c)	$S_c = d_{ins}/d_{cir} = r_{ins}/r_{cir}$	The ratio of the diameter of the largest inscribed circle of the particle (d_{ins}) to the smallest circumscribed circle of the particle (d_{cir})	Santamarina and Cho 2004
Diameter sphericity (S_d)	$S_d = d_e/d_{cir}$	The ratio of the diameter of a circle having the same area as the original particle (d_e) to the diameter of the minimum circumscribing circle (d_{cir})	Wadell 1935
Area sphericity (S_a)	$S_a = A/A_{cir} = d_e^2/d_{cir}^2$	The ratio of the area of the particle (A) to the area of the smallest circumscribing circle ($A_{cir} = \frac{\pi d_{cir}^2}{4}$)	Riley 1941
ASTM Roundness /ISO Roundness /Image J Roundness (R_{ASTM})	$R_{ASTM} = A/A_{Fmax} = d_e^2/d^2_{Fmax}$	The ratio of the area of the particle (A) to the area of the circle with a diameter equals to maximum Feret value ($A_{Fmax} = \frac{\pi d_{Fmax}^2}{4}$)	ASTM F1877-16/ISO 9276-6

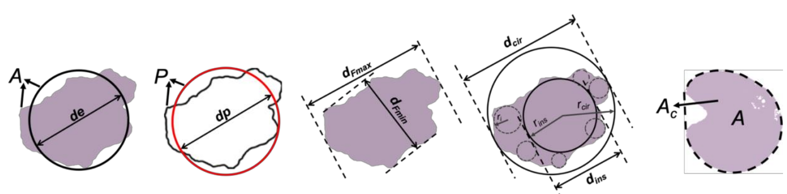

- **Roundness** and **sphericity** are the most commonly used shape descriptors.
- Barrett (1980) claimed that R_{wadell} describes particle shape at an intermediate scale, which reflects the abrasion and formation of a particle.
- Definitions of roundness may operate at different particle scales, such as R_{ASTM} and Circularity.
- Sphericity terms are also in common use, which are not necessarily correlated with R_{wadell} or R_{ASTM}.
- Correlation analysis of roundness pairs may facilitate analysis of the particle formation process.

6 Comparison of shape descriptors for determining roundness

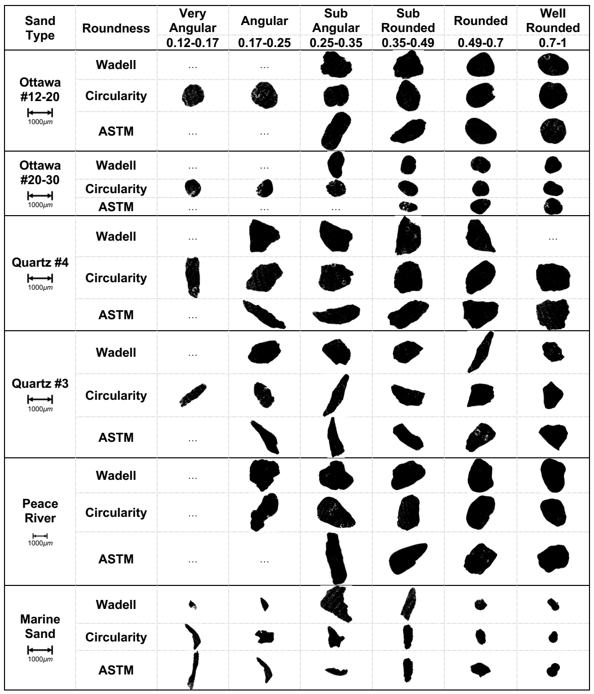

R_{wadell}, Circularity and R_{ASTM} according to Power's chart

- Variations of particle shape from very angular to well rounded are different depending on the selected roundness parameter.
- R_{wadell} reflects changes of roundness at the corner.
- R_{ASTM} describes particle overall shape and reflects variations in the proportions of the particle from elongated to rounded.
- Cr focuses on the smoothness of the particle's perimeter.
- R_{wadell}, Circularity and R_{ASTM} are conceptually distinct, measuring different aspects of sand morphology.

6 Evaluation of roundness parameters in use for sand

Pearson correlation of shape descriptors

Ottawa #12-20

Shape descriptor	R_{wadell}	Cx	S_p	Cr	AR	S_c	S_d	S_a	R_{ASTM}
ASTM Roundness, R_{ASTM}	0.29	0.33	0.24	0.24	0.96	0.96	1	1	1
Area sphericity, S_a	0.32	0.35	0.26	0.25	0.95	0.97	1	1	
Diameter sphericity, S_d	0.32	0.36	0.26	0.25	0.94	0.97	1		
Circle ratio sphericity, S_c	0.28	0.34	0.26	0.26	0.95	1			
Aspect Ratio, AR	0.14	0.14	0.11	0.11	1				
Circularity, Cr	0.46	0.72	1	1					
Perimeter Sphericity, S_p	0.47	0.75	1						
Convexity, Cx	0.53	1							
Wadell Roundness, R_{wadell}	1								

Quartz #3

Shape descriptor	R_{wadell}	Cx	S_p	Cr	AR	S_c	S_d	S_a	R_{ASTM}
ASTM Roundness, R_{ASTM}	-0.09	0.34	0.48	0.49	0.95	0.96	0.99	0.99	1
Area sphericity, S_a	-0.09	0.35	0.48	0.52	0.94	0.97	1	1	
Diameter sphericity, S_d	-0.09	0.35	0.5	0.5	0.94	0.97	1		
Circle ratio sphericity, S_c	-0.12	0.37	0.5	0.5	0.95	1			
Aspect Ratio, AR	-0.16	0.2	0.4	0.41	1				
Circularity, Cr	0.05	0.62	1	1					
Perimeter Sphericity, S_p	0.05	0.62	1						
Convexity, Cx	0.13	1							
Wadell Roundness, R_{wadell}	1								

Ottawa #20-30

Shape descriptor	R_{wadell}	Cx	S_p	Cr	AR	S_c	S_d	S_a	R_{ASTM}
ASTM Roundness, R_{ASTM}	0.28	0.34	0.31	0.31	0.96	0.92	0.99	0.99	1
Area sphericity, S_a	0.31	0.35	0.32	0.12	0.95	0.93	1	1	
Diameter sphericity, S_d	0.31	0.36	0.33	0.33	0.94	0.93	1		
Circle ratio sphericity, S_c	0.26	0.34	0.35	0.33	0.95	1			
Aspect Ratio, AR	0.15	0.16	0.18	0.18	1				
Circularity, Cr	0.32	0.81	1	1					
Perimeter Sphericity, S_p	0.32	0.82	1						
Convexity, Cx	0.35	1							
Wadell Roundness, R_{wadell}	1								

Peace River

Shape descriptor	R_{wadell}	Cx	S_p	Cr	AR	S_c	S_d	S_a	R_{ASTM}
ASTM Roundness, R_{ASTM}	0.04	0.28	0.26	0.26	0.94	0.96	0.99	0.99	1
Area sphericity, S_a	0.07	0.3	0.27	0.27	0.94	0.96	1	1	
Diameter sphericity, S_d	0.06	0.3	0.28	0.27	0.94	0.96	1		
Circle ratio sphericity, S_c	0.06	0.35	0.27	0.27	0.94	1			
Aspect Ratio, AR	-0.09	0.13	0.18	0.18	1				
Circularity, Cr	0.2	0.51	1	1					
Perimeter Sphericity, S_p	0.2	0.52	1						
Convexity, Cx	0.47	1							
Wadell Roundness, R_{wadell}	1								

Quartz #4

Shape descriptor	R_{wadell}	Cx	S_p	Cr	AR	S_c	S_d	S_a	R_{ASTM}
ASTM Roundness, R_{ASTM}	-0.29	0.4	0.41	0.41	0.95	0.96	0.99	0.99	1
Area sphericity, S_a	-0.27	0.42	0.42	0.42	0.93	0.97	1	1	
Diameter sphericity, S_d	-0.28	0.43	0.43	0.42	0.93	0.97	1		
Circle ratio sphericity, S_c	-0.31	0.43	0.42	0.42	0.94	1			
Aspect Ratio, AR	-0.39	0.24	0.35	0.35	1				
Circularity, Cr	-0.1	0.51	1	1					
Perimeter Sphericity, S_p	-0.1	0.52	1						
Convexity, Cx	0.16	1							
Wadell Roundness, R_{wadell}	1								

Marine Sand

Shape descriptor	R_{wadell}	Cx	S_p	Cr	AR	S_c	S_d	S_a	R_{ASTM}
ASTM Roundness, R_{ASTM}	0.53	0.59	0.61	0.61	0.96	0.97	0.99	1	1
Area sphericity, S_a	0.54	0.6	0.62	0.63	0.94	0.97	0.99	1	
Diameter sphericity, S_d	0.51	0.61	0.62	0.61	0.95	0.97	1		
Circle ratio sphericity, S_c	0.48	0.62	0.63	0.62	0.93	1			
Aspect Ratio, AR	0.4	0.39	0.45	0.45	1				
Circularity, Cr	0.43	0.79	1	1					
Perimeter Sphericity, S_p	0.41	0.83	1						
Convexity, Cx	0.35	1							
Wadell Roundness, R_{wadell}	1								

- Correlation analysis was able to classify siliceous sand into naturally sorted or crushed:
  - *Crushed quartz*: a negative correlation: R_{wadell} and AR; weak correlation: R_{wadell} and Cx, S_p
  - *Naturally sorted sand*: positive or no correlation: R_{wadell} and AR; moderate to strong correlation: R_{wadell} and Cx, S_p
- AR is the main impacted shape descriptor capturing the evolution of crushing for quartz sand.
- Marine Sand exhibits relatively high correlation coefficients, complex formation process is different from other sands.

6 Evaluation of roundness parameters in use for sand

- **Shape descriptors** are categorized into four groups according to their correlation and independence:
  - *Larger-scale descriptors*: AR, S_a, S_d, S_c, and R_{ASTM}
  - *Perimeter descriptors:* S_p and Cr
  - *Roundness descriptor*: R_{wadell}
  - *Convexity descriptor:* Cx

Check for updates

ASCE

Evaluation of Roundness Parameters in Use for Sand

Linzhu Li, S.M.ASCE[1]; and Magued Iskander, Ph.D., P.E., F.ASCE[2]

Abstract: Particle granulometry plays an important role in the engineering behavior of many sands. However, the evaluation of particle shape and size has historically been a tedious and labor-intensive process. The recent availability of dynamic image analysis (DIA) makes it possible to evaluate many particle shape and size parameters, quickly and conveniently. These shape parameters include sphericity, roundness, aspect ratio, circularity, and convexity; while size descriptors include the diameter of a circle of equal projection area (EQPC), a variety of Feret diameters, as well as inscribed and circumscribed circle diameters. The terms *roundness* and *sphericity* are commonly used to describe how close a particle resembles a sphere, with many definitions in common use. However, it is not immediately evident how these roundness descriptors correlate. The correlation of nine shape and six size descriptors was investigated for six sands that reflect the breadth of particle shapes and sizes that may be encountered. The analysis was based on 1,000 images of each sand obtained using two-dimensional DIA apparatus. The study demonstrates that there is no correlation between size and shape parameters, and that shape descriptors can be reduced to four independent shape parameters representing the granulometry of sand at different scales. The use of size and shape descriptors for classification of sand was explored using six machine learning algorithms including support vector machines (SVMs), random forest, decision tree, bagging tree, *k*-nearest neighbors (KNN), and bagging KNN. Classification accuracies of 77% and 66% were achieved using size and shape features, respectively. The mean accuracy improved to 87% when combining both size and shape descriptors using bagging KNN and random forest classifiers. The analysis also revealed an important hierarchy of size and shape features employed, with EQPC and Wadell's roundness alone classifying sands with 70% accuracy. **DOI: 10.1061/(ASCE)GT.1943-5606.0002585.** © *2021 American Society of Civil Engineers.*

Author keywords: Roundness; Sphericity; Pearson correlation; Cross-validation; Aspect ratio; Circularity; Convexity; Support vector machines (SVMs); Random forest; Decision tree; Bagging tree; *k*-nearest neighbors (KNN); Bagging KNN.

Introduction

Previous studies have shown that particle size and shape significantly influence the mechanical behavior of granular soils, including packing density, shear strength, void ratio, friction angle, and hydraulic conductivity (e.g., Cho et al. 2006; Rousé et al. 2008; Bareither et al. 2008; Cabalar and Akbulut 2016; Zheng and Hryciw 2016). Size and shape are two fundamental properties of sedimentary particles, yielding a variety of information about depositional history, abrasion, transport processes, and sediment source areas (Sherman et al. 2013). Wadell (1932, 1933) introduced the measurement of two-dimensional (2D) projection of particle shape as a practical representation of three-dimensional (3D) particle morphology. The method is believed to not cause significant bias and is still in use today. In recent years, dynamic image analysis (DIA) has been increasingly applied for characterizing particle size and shape of sand (e.g., Altuhafi et al. 2013; Wang et al. 2019; Suescun-Florez et al. 2020; Li et al. 2021). DIA employs a high-frame-rate camera to image a large number of individual particles of sand in a short time and provides various 2D size and shape descriptors, efficiently and quickly, including aspect ratio (AR), convexity, sphericity, and roundness of millions of particles (Li and Iskander 2020). However, there is no general agreement on which of these size and shape descriptors should be used either to classify sand particles or trace its sedimentary source.

Roundness and sphericity are the most commonly used shape descriptors to characterize particle morphology and a number of equations have been proposed to capture the particle's essence (Table 1). Barrett (1980) claimed that Wadell roundness (R_{wadell}) describes particle shape at an intermediate scale, which reflects the abrasion and formation of a particle. However other definitions of roundness may operate at different particle scales. For example, ASTM F1877's (ASTM 2016) definition of roundness (R_{ASTM}), which is also shared with ISO 9276-6 (ISO 2008) and the influential Image J version 1.53h software, captures a larger scale than that of R_{wadell}. The definition R_{ASTM} has been adopted in many studies including Wei et al. (2020) and Maroof et al. (2020). A third definition of roundness was introduced by Cox (1927), but it is more commonly known as circularity. Cox's definition has been adopted by several studies including Nakata et al. (2001) and Altuhafi et al. (2016). In addition, a variety of sphericity terms are also in common use (Table 1), which are not necessarily correlated with R_{wadell} or R_{ASTM}. This might cause terminological confusion, in that these parameters classify different aspects of particle morphology. It is therefore of interest to examine the correlation between the various roundness parameters in use for characterizing sand particle shape. At the same time, correlation analysis of roundness pairs may facilitate analysis of the particle formation process.

Six types of sand including naturally occurring silica sand, crushed quartz, feldspathic sand, and a calcareous sediment were investigated. These sand particles differ in size and shape, varying

[1]School of Engineering Fellow, Dept. of Civil and Urban Engineering, New York Univ. Tandon School of Engineering, 6 Metrotech Center, Brooklyn, NY 11201. Email: LL3256@nyu.edu

[2]Professor and Chair, Dept. of Civil and Urban Engineering, New York Univ. Tandon School of Engineering, 6 Metrotech Center, Brooklyn, NY 11201 (corresponding author). ORCID: https://orcid.org/0000-0001-8245-1451. Email: Iskander@nyu.edu

Note. This manuscript was submitted on September 1, 2020; approved on April 5, 2021; published online on June 16, 2021. Discussion period open until November 16, 2021; separate discussions must be submitted for individual papers. This paper is part of the ***Journal of Geotechnical and Geoenvironmental Engineering***, © ASCE, ISSN 1090-0241.

7 Use of machine learning methods for sand classification

Features - Engineering size and shape descriptors

Descriptors	Formula	Definition	Reference
EQPC	d_e	Diameter of a Circle of Equal Projection Area	ASTM F1877-16
Feret-max	d_{Fmax}	Maximum Feret diameter	Kuo and Freeman 2000
Feret-min	d_{Fmin}	Minimum Feret diameter	
MIC diameter	$d_{ins} = 2r_{ins}$	Maximum inscribed circle diameter	Santamarina and Cho 2004
MCC diameter	$d_{cir} = 2r_{cir}$	Minimum circumscribed circle diameter	
PED diameter	d_p	Diameter of a Circle of Equal Perimeter	ISO 9276-6 2008
Wadell Roundness (R_{wadell})	$R_{wadell} = \frac{\sum_{i=1}^{N} \frac{r_i}{N}}{r_{ins}}$	The ratio of the average radius of corner circles of the particle to the radius of the maximum inscribed circle	Wadell 1932
Convexity (Cx) (aka. Solidity)	$Cx = A/A_c$	The ratio between the real particle area (A) and the area of the convex hull (A_c) (Fig.2)	Mora and Kwan 2000
Perimeter Sphericity (S_p)	$S_p = P_e/P = d_e/d_p$	The ratio of the perimeter of the area equivalent circle, P_e, to the real perimeter, P	ISO 9276-6 2008
Aspect Ratio (AR) (aka. Wadell's Sphericity)	$AR = d_{Fmin}/d_{Fmax}$	The ratio of the width of the particle (d_{Fmin}) to the length of particle (d_{Fmax})	ISO 9276-6 2008

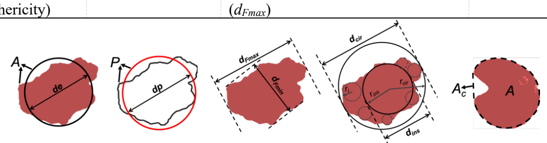

Employed 6 size and 4 shape descriptors

- Engineering size and shape descriptors can be easily obtained from image dataset obtained using DIA.
- **Size & Shape descriptors can be trained in ML models**
- ML techniques may eventually assist engineers on-site to quickly determine geotechnical properties of soil formations that would presently be analyzed in laboratories.

7 Use of machine learning methods for sand classification

Nine types of sands

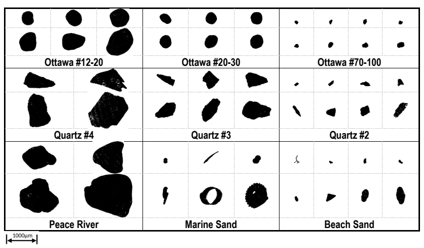

Sand	Particle size diameter D_{50} (µm) of *indicated Size Descriptor*						Statistics	Particle shape descriptor			
	d_e	d_{Fmax}	d_{Fmin}	d_{ins}	d_{cir}	d_p		R_{wadell}	Cx	S_p	AR
Ottawa #12-20	1097	1271	1013	946	1276	1617	Mean	0.73	0.96	0.70	0.79
							Median	0.75	0.96	0.70	0.80
							St. Dev.	0.12	0.02	0.10	0.10
Ottawa #20-30	820	942	745	701	945	1027	Mean	0.78	0.96	0.79	0.79
							Median	0.79	0.97	0.80	0.79
							St. Dev.	0.09	0.02	0.09	0.09
Ottawa #70-100	285	352	259	228	354	371	Mean	0.75	0.91	0.76	0.73
							Median	0.76	0.92	0.78	0.73
							St. Dev.	0.10	0.05	0.10	0.11
Quartz #4	1742	2405	1477	1319	2420	2835	Mean	0.38	0.93	0.62	0.62
							Median	0.38	0.93	0.62	0.62
							St. Dev.	0.08	0.03	0.09	0.14
Quartz #3	1011	1386	853	756	1400	1409	Mean	0.43	0.89	0.69	0.61
							Median	0.43	0.90	0.71	0.62
							St. Dev.	0.09	0.05	0.10	0.15
Quartz #2	321	461	266	228	465	464	Mean	0.57	0.82	0.70	0.63
							Median	0.58	0.83	0.72	0.64
							St. Dev.	0.12	0.08	0.12	0.15
Peace River	2162	2711	1881	1745	2722	3111	Mean	0.50	0.96	0.70	0.71
							Median	0.50	0.96	0.70	0.72
							St. Dev.	0.11	0.02	0.08	0.12
Marine Sand	422	580	370	307	583	680	Mean	0.62	0.87	0.62	0.65
							Median	0.61	0.89	0.64	0.68
							St. Dev.	0.17	0.07	0.13	0.17
Beach Sand	255	354	219	183	355	389	Mean	0.67	0.86	0.67	0.65
							Median	0.68	0.88	0.69	0.65
							St. Dev.	0.13	0.07	0.12	0.14

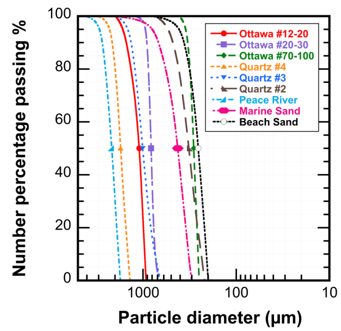

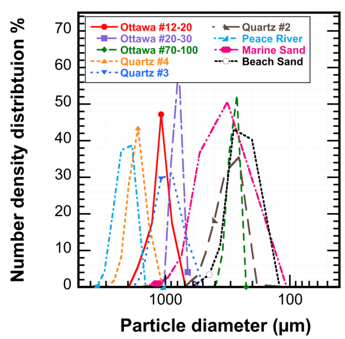

Particle size distribution

Investigated sand specimen:

- Two-thousand particle images.
- Identifying each sand by size alone is difficult due to overlapping sizes among various sands.
- Slightly shape differences exist in similar sand types.
- Quantified particle size and shape features could aid with the classification of materials and serve to substitute subjective visual observations.

7 Mean classification accuracy use 10-fold cross-validation

classifiers	Features	Support Vector Machines (SVM)	Decision Tree	Naïve Bayes	K-nearest Neighbors (KNN)	Neural Network (MLP)	Random Forest	Ensemble voting
Accuracy	Size	0.69	0.59	0.59	0.65	**0.73**	0.65	0.69
	Shape	0.57	0.45	0.50	0.56	**0.58**	0.55	0.57
	Size and shape	0.74	0.67	0.71	0.73	**0.75**	0.73	**0.75**

- Five individual ML classifiers and two ensemble methods.
- Data preprocessing: *Normalization* and *Standardization*.
- Hyperparameters optimization: *Grid search* optimizer.
- Accuracy:
  - size descriptor > shape descriptors (66% vs 54%)
  - **Size + shape: 75% Neural network and Ensemble voting**
  - Decision tree method is not suggested.
- Efficiency: a few seconds to 3 minutes on a personal computer.

7 Use of machine learning methods for sand classification

Features – Scale-invariant feature transform (SIFT)

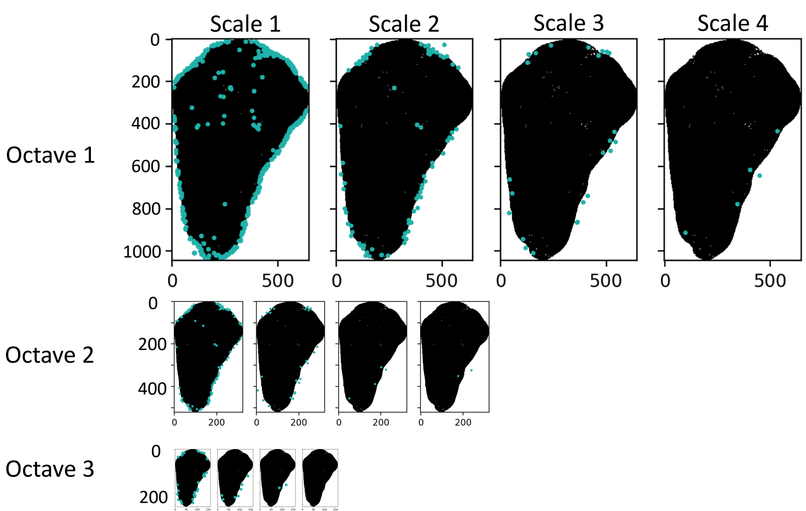

The *Gaussian Pyramid* and detected SIFT keypoints for a typical sand image. Each row contains particle images with increasing Gaussian blurring, images in each column are down sampled to half the size of the previous row.

- SIFT features permit sand classification using images having different resolutions and scales.
- *Keypoint Descriptors*: calculated using a histogram of oriented gradients (HOG).
    - *Magnitude*: $m(x,y) = \sqrt{(L(x+1,y) - L(x-1,y))^2 + (L(x,y+1) - L(x,y-1))^2}$
    - *Direction*: $\theta(x,y) = \tan^{-1}\frac{L(x,y+1)-L(x,y-1)}{L(x+1,y)-L(x-1,y)}$
- 8 bin orientation histogram is created for each keypoint and each keypoint descriptor is represented as a feature vector of 128 bin values (16 sub blocks × 8 orientations)

7 SIFT features of two particles

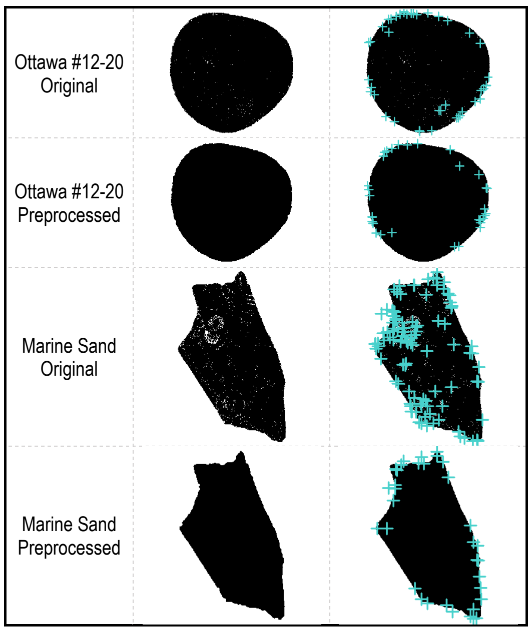

SIFT keypoints

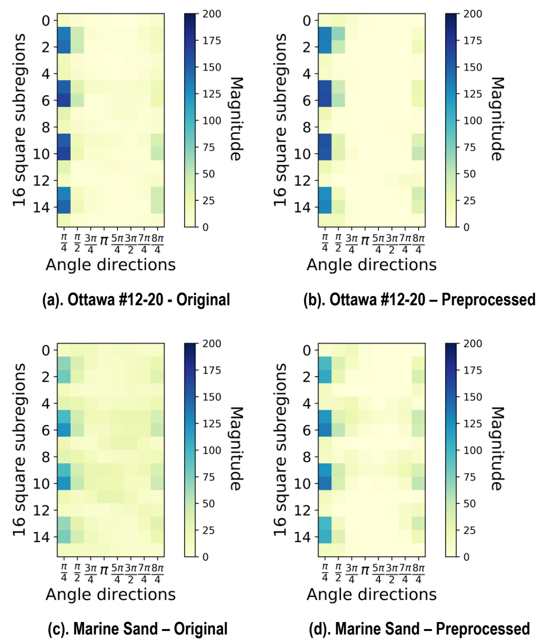

Average of orientation histograms of all SIFT keypoints for the two particles

- Two types of image dataset: original images and Solid black particles.
  - White dots inside each image could be related to materials properties.
  - Size and shape descriptors analyze particle outline.
- *Marine Sand*: HOG more diversity due to highly irregular particle shape.
- *Ottawa #12-20*: HOG concentrated at $\pi/4$, $\pi/2$ and 2π.

7 SIFT features of nine types of sands

- ➢The HOG represents the average of all identified SIFT keypoints in 2000 particles.
- ➢Each sand possesses a distinctive SIFT direction and magnitude.
- ➢The retained SIFT keypoints in each image represent high contrast pixels that can consequently be trained as features to distinguish sands.

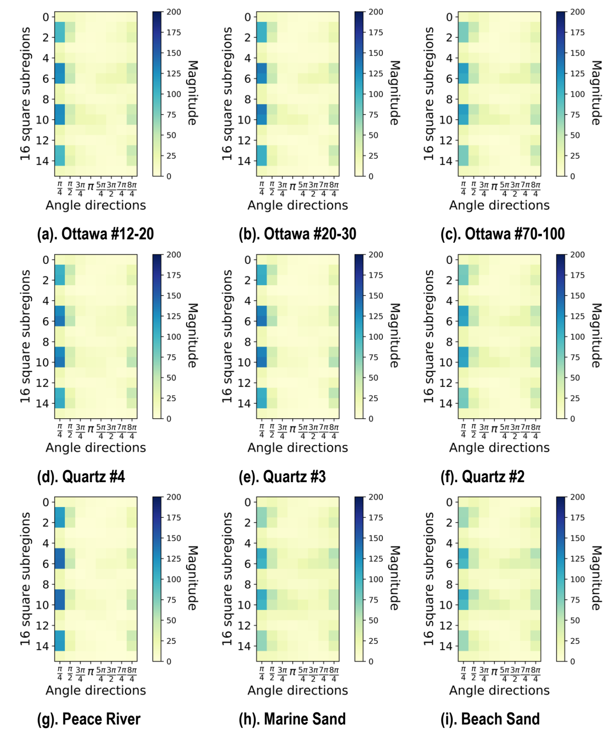

Average of orientation histograms of all SIFT keypoints

7 Correlation between SIFT & shape descriptors

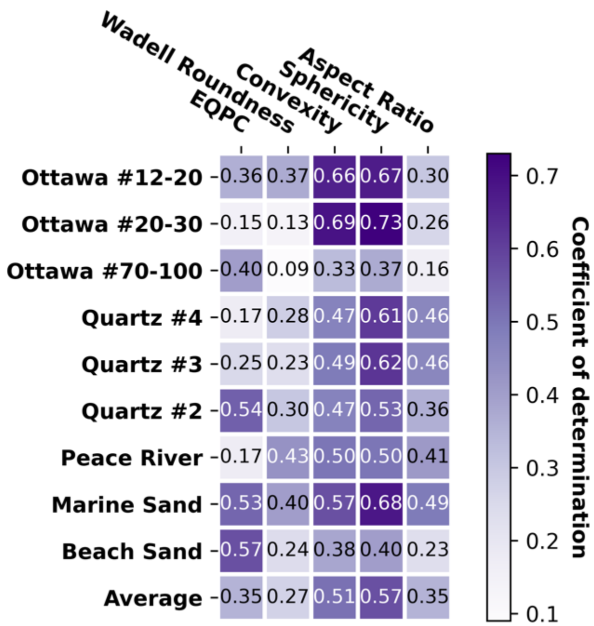

(a) Original images

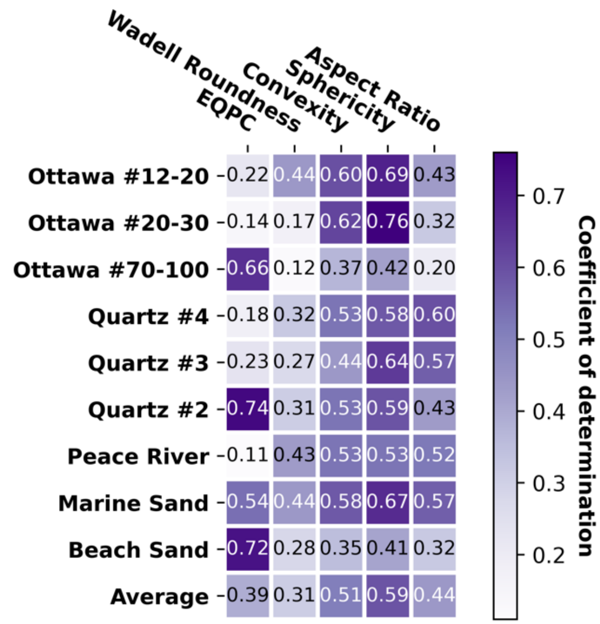

(b) Preprocessed images

Correlation between 128-dimension SIFT keypoints and size and shape descriptors

- Multiple linear regression (MLR)
- Moderate correlations exist between SIFT and Sphericity and Convexity.
- Sphericity and Convexity capture the overall smoothness and compactness of particle perimeters at a finer scale, perhaps similar to the HOG in SIFT.
- Preprocessed images have a higher correlation to shape descriptors.

7 Correlation between number of SIFT keypoints and shape descriptors

- ➢Number of SIFT keypoints depends on the original image size (all images preprocessed as uniform size 300 × 300 pixels).
- ➢Preprocessed images have fewer keypoints
- ➢Convexity and Sphericity were inversely proportional to the number of SIFT Keypoints.
- ➢Number of keypoints are not correlated to *AR* and R_{wadell}.

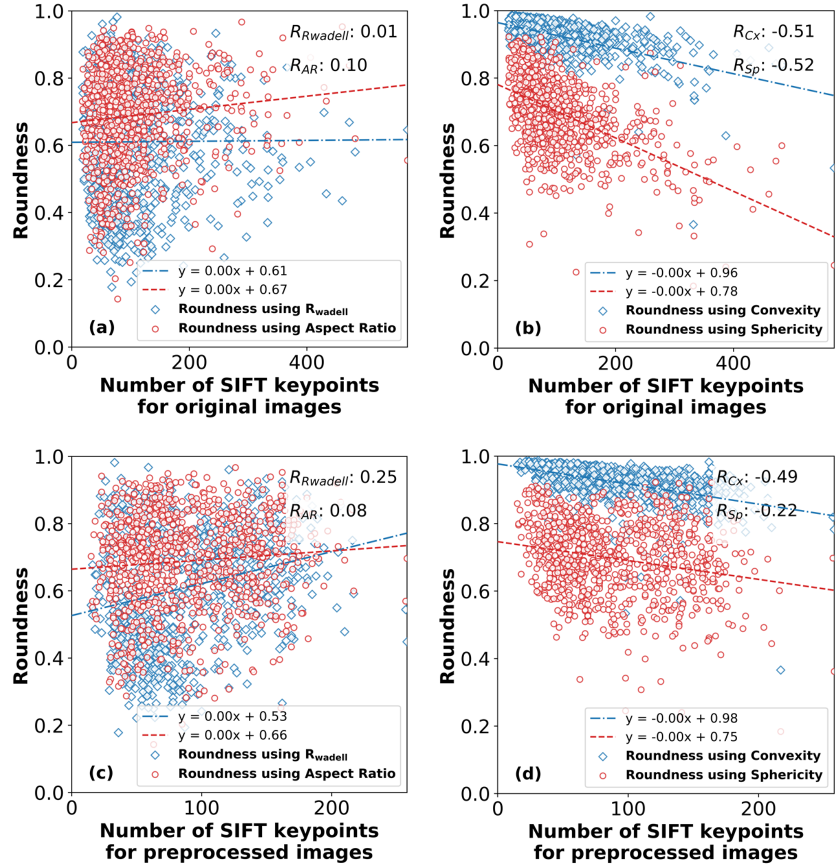

7 Bag of features used in classification

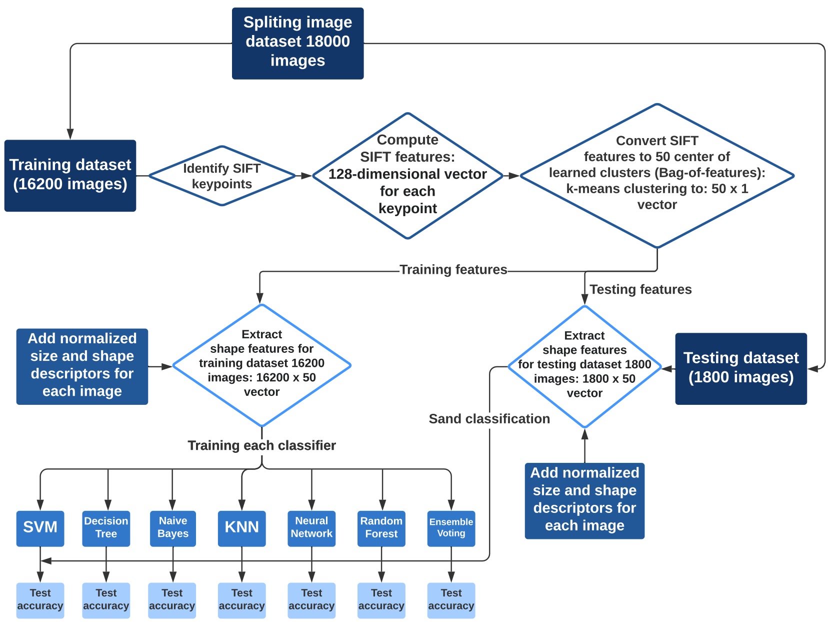

Flowchart of image classification using features extracted by SIFT algorithm and BOF

- **Bag of features (BOF)** improves the efficiency of training models by reducing feature dimensionality.
- The SIFT features extracted for 18,000 images took 40 minutes on a PC having 32GB of RAM and an Intel core i7-9700 CPU.
- Two smaller datasets comprising 1000 original and preprocessed images were compared, operation time 14 mins to extract SIFT.
- The time used for training and testing 18000 data in SIFT is ~2-3 that required for using size and shape descriptors.

7 Mean classification accuracy using SIFT features (10-fold Cross-validation)

classifiers	Image dataset	Features	Support Vector Machines (SVM)	Decision Tree	Naïve Bayes	K-nearest Neighbors (KNN)	Neural Network MLP	Random Forest	Ensemble Voting
Analysis using 18,000 images (2000 images each sand x 9 sands)									
Accuracy	Original images	SIFT	**0.55**	0.36	0.32	0.50	0.53	0.52	0.53
		Size, SIFT	**0.73**	0.64	0.55	0.65	**0.73**	**0.73**	**0.73**
		Size, Shape, SIFT	0.81	0.72	0.66	0.76	0.80	**0.83**	0.81
Accuracy	Processed images	SIFT	**0.52**	0.37	0.43	0.47	0.50	0.50	0.51
		Size, SIFT	**0.74**	0.65	0.66	0.66	0.72	**0.74**	**0.74**
		Size, Shape, SIFT	**0.81**	0.72	0.74	0.75	0.77	0.80	**0.81**
Analysis using 9000 images (1000 images each sand x 9 sands)									
Accuracy	Original images	SIFT	**0.55**	0.35	0.32	0.48	0.53	0.52	0.53
		Size, SIFT	0.72	0.64	0.55	0.65	0.72	**0.73**	0.72
		Size, Shape, SIFT	0.79	0.71	0.66	0.74	0.77	**0.82**	0.80
Accuracy	Processed images	SIFT	**0.51**	0.38	0.43	0.46	0.49	0.48	0.49
		Size, SIFT	**0.73**	0.64	0.66	0.65	0.71	**0.73**	**0.73**
		Size, Shape, SIFT	0.78	0.72	0.75	0.72	0.75	**0.81**	0.79

- **Classification accuracy:**
  - SIFT (32-55%) < Shape (45-58%).
  - Size and SIFT features (55-73%) < size and shape features (67-75%).
  - Using size, shape and SIFT, 83% accuracy was obtained using Random Forest classifier.
  - No significant difference between original and preprocessed images
  - A slightly lower accuracy (<2%) was achieved by using 9000 images.

7 SIFT: Summary and Conclusions

- **Neural Network** provided the best performance for classifying 73%, 58% and 75% of sand particles using size, shape, size and shape descriptors.
- The use of SIFT features alone can identify up to **55%** of sand particles, while using size and SIFT features can provide **73%** accuracy. These values are consistently **2-3%** smaller than using size and shape descriptors.
- Image preprocessing was found **counterproductive**.


Acta Geotechnica
Use of Machine Learning Methods for Classification of Sand Particles
--Manuscript Draft--

Manuscript Number:	AGEO-D-21-00669
Full Title:	Use of Machine Learning Methods for Classification of Sand Particles
Article Type:	Original Research Paper
Keywords:	Krumbein-Sloss; Support Vector Machines; Bag of Features; K-means; Clustering; Ensemble; Cross Validation
Corresponding Author:	Magued Iskander, PhD, PE, F.ASCE New York University Tandon School of Engineering Brooklyn, New York UNITED STATES
Corresponding Author Secondary Information:	
Corresponding Author's Institution:	New York University Tandon School of Engineering
Corresponding Author's Secondary Institution:	
First Author:	Linzhu Li, MSc
First Author Secondary Information:	
Order of Authors:	Linzhu Li, MSc
	Magued Iskander, PhD, PE, F.ASCE
Order of Authors Secondary Information:	
Funding Information:	
Abstract:	Particle classification is essential for geotechnical engineering practice since particle shapes correlate with the mechanical and hydraulic properties of sand layers. Traditional shape classification is tedious, subjective, and time consuming because it depends on manual visual comparison with reference particles. This study demonstrates the feasibility of employing machine learning algorithms for sand classification . Machine Learning (ML) models are increasingly being introduced for automatic identification and classification of various objects. Nine types of sand were selected, and the analysis was based on 2000 binary images of each sand that were obtained from Dynamic Image Analysis (DIA). Each particle was represented by six engineering size and four shape descriptors. The efficacy of seven ML models for automatically classifying individual sand particles was explored. The study demonstrates that the size and shape descriptors are efficient and robust to identify up to 75% of sand particles, using a Neural Network classifier. In addition, use of Scale Invariant Feature Transform (SIFT) features was also explored to permit future generalization of sand classification using image datasets containing images with different scales and resolutions. Adding SIFT to size and shape can increase classification accuracy to 83% using a Random Forest classifier. The analysis also reveals that Histograms of Orientation Gradients of SIFT keypoints in sand appear well correlated with Sphericity and Convexity of particles. This study suggests that a dataset of 2000 particles per sand is sufficient for optimal classification performance, and that image pre-processing of DIA images was not necessary.

Conclusions

- **DIA** can be used for routine analysis of regular particles
  - Faster and more accurate than Sieve analysis
  - DIA needs to be supplemented by µCT for very complex particles

- ML promises to become commonly employed for routine classification of sand from ordinary images, a voting algorithm can be used to classify the material based on the classification of the majority of individual particles.
  - Shape & Size descriptors provide suitable representation of particle granulometry
  - SIFT can help with databases of images having various scales

Publications

	Journal articles
1.	**Li, L.,** & Iskander, M. (2020). Evaluation of Dynamic Image Analysis for Characterizing Granular Soils. *Geotechnical Testing Journal*, DOI: 10.1520/GTJ20190137.
2.	**Li, L.,** Beemer, R. & Iskander, M. (2021). Granulometry of Two Marine Calcareous Sands. *Journal of geotechnical and geoenvironmental engineering*, DOI:10.1061/(ASCE)GT.1943-5606.0002431.
3.	**Li, L.,** & Iskander, M. (2021). Comparison of 2D and 3D Dynamic Image Analysis for Characterization of Natural Sands. *Engineering Geology, DOI:10.1016/j.enggeo.2021.106052.*
4.	**Li, L.,** & Iskander, M. (2021). Evaluation of Roundness Parameters in use for Sand. *Journal of geotechnical and geoenvironmental engineering,* DOI:10.1061/(ASCE)GT.1943-5606.0002585.
5.	**Li, L.,** Sun, Q., & Iskander, M. (2021). Evaluation of 3D Dynamic Image Analysis For Characterization of Natural Sands. *Geotechnique*. (In press)
6.	**Li, L.,** & Iskander, M. (2021). Use of Machine Learning Methods for Classification of Sand Particles. *Acta Geotechnica*. (Submitted).
	Conference papers
1.	**Li, L.,** Iskander, M., & Omidvar, M. (2018, July). Visualisation of inter-granular pore fluid flow. In *Physical Modelling in Geotechnics*, Volume 2: Proceedings of the 9th International Conference on Physical Modelling in Geotechnics (ICPMG 2018), London, United Kingdom (p. 859).
2.	**Li, L.,** Omidvar, M., Bless, S., & Iskander, M. (2019, March). Visualizing the Role of Particle Shape on 2D Inter-Particle Fluid Flow Using a Transparent Soil Surrogate. In *Geo-Congress 2019: Geotechnical Materials, Modeling, and Testing (pp. 618-627)*. DOI: 10.1061/9780784482124.063.
3.	Machairas, N., **Li, L.,** & Iskander, M. (2020, February). Application of Dynamic Image Analysis to Sand Particle Classification Using Deep Learning. In *Geo-Congress 2020: Modeling, Geomaterials, and Site Characterization (pp. 612-621)*. DOI: 10.1061/9780784482803.065.

Thank you

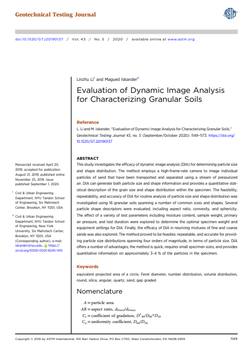
Geotechnical Testing Journal

Evaluation of Dynamic Image Analysis for Characterizing Granular Soils


Granulometry of Two Marine Calcareous Sands

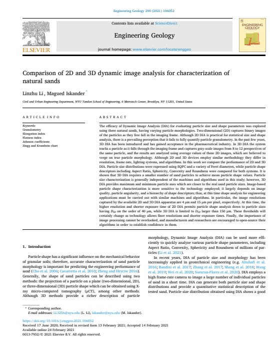
Engineering Geology

Comparison of 2D and 3D dynamic image analysis for characterization of natural sands


Evaluation of Roundness Parameters in Use for Sand

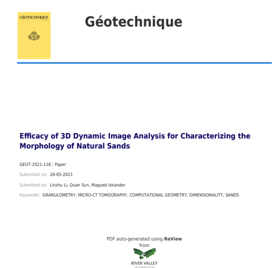
Géotechnique

Efficacy of 3D Dynamic Image Analysis for Characterizing the Morphology of Natural Sands

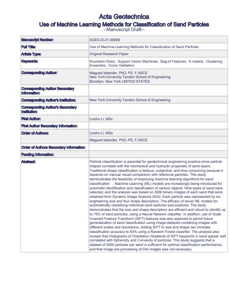
Acta Geotechnica

Use of Machine Learning Methods for Classification of Sand Particles